

FGFR1-Frs2/3 Signalling Maintains Sensory Progenitors during Inner Ear Hair Cell Formation

Kazuya Ono^{1,2}, Tomoko Kita¹, Shigeru Sato³, Paul O'Neill¹, Siu-Shan Mak¹, Marie Paschaki¹, Masataka Ito⁴, Noriko Gotoh⁵, Kiyoshi Kawakami³, Yoshiki Sasai², Raj K. Ladher^{1*}

1 Sensory Development, RIKEN Center for Developmental Biology, Chuo-ku, Kobe, Japan, **2** Neurogenesis and Organogenesis, RIKEN Center for Developmental Biology, Chuo-ku, Kobe, Japan, **3** Division of Biology, Center for Molecular Medicine, Jichi Medical University, Shimotsuke, Tochigi, Japan, **4** Department of Anatomy, National Defense Medical College, Tokorozawa, Japan, **5** Division of Genetics, Institute of Medical Science, University of Tokyo, Minato-ku, Japan

Abstract

Inner ear mechanosensory hair cells transduce sound and balance information. Auditory hair cells emerge from a Sox2-positive sensory patch in the inner ear epithelium, which is progressively restricted during development. This restriction depends on the action of signaling molecules. Fibroblast growth factor (FGF) signalling is important during sensory specification: attenuation of *Fgfr1* disrupts cochlear hair cell formation; however, the underlying mechanisms remain unknown. Here we report that in the absence of FGFR1 signaling, the expression of Sox2 within the sensory patch is not maintained. Despite the down-regulation of the prosensory domain markers, p27^{Kip1}, *Hey2*, and *Hes5*, progenitors can still exit the cell cycle to form the zone of non-proliferating cells (ZNPC), however the number of cells that form sensory cells is reduced. Analysis of a mutant *Fgfr1* allele, unable to bind to the adaptor protein, *Frs2/3*, indicates that Sox2 maintenance can be regulated by MAP kinase. We suggest that FGF signaling, through the activation of MAP kinase, is necessary for the maintenance of sensory progenitors and commits precursors to sensory cell differentiation in the mammalian cochlea.

Citation: Ono K, Kita T, Sato S, O'Neill P, Mak S-S, et al. (2014) FGFR1-Frs2/3 Signalling Maintains Sensory Progenitors during Inner Ear Hair Cell Formation. *PLoS Genet* 10(1): e1004118. doi:10.1371/journal.pgen.1004118

Editor: Kathryn S. E. Cheah, The University of Hong Kong, Hong Kong

Received: May 10, 2013; **Accepted:** December 2, 2013; **Published:** January 23, 2014

Copyright: © 2014 Ono et al. This is an open-access article distributed under the terms of the Creative Commons Attribution License, which permits unrestricted use, distribution, and reproduction in any medium, provided the original author and source are credited.

Funding: This work was supported by JSPS Studentship (<http://www.jsps.jp>) to KO and a RIKEN CDB intramural grant. The funders had no role in study design, data collection and analysis, decision to publish, or preparation of the manuscript.

Competing Interests: The authors have declared that no competing interests exist.

* E-mail: raj-ladher@cdb.riken.jp

Introduction

The mammalian cochlea transduces sound using a dedicated sensory organ, the organ of Corti, which comprises of a highly ordered array of mechanosensory hair cells (HCs) and their associated support cells (SCs). The arrangement of cochlear HCs, 3 rows of outer hair cells (OHCs) and one row of inner hair cells (IHCs), together with SCs results from a balance between specification, progenitor expansion and differentiation [1].

The first step in HC specification is the induction of a Sox2-positive territory known as the sensory patch. Sox2 is critical for neurosensory precursor formation in the inner ear [2–4] and is induced by Notch signalling through its ligand Jagged (*Jag1*) [5–9]. BMP signalling [10] then specifies the prosensory domain, the immediate precursors of the HCs and SCs, from within this Sox2-positive sensory patch. At specification, the prosensory domain exits the cell cycle, expressing the cell cycle inhibitor p27^{Kip1} as well as other prosensory domain markers. Importantly, the prosensory domain first becomes post-mitotic at the apical end of the cochlea from E12.5, spreading basally until E14.5 [11,12].

HCs and SCs are picked out from within the prosensory domain through Notch signalling from putative SCs, acting on Delta1 or *Jag2* in potential HCs [5,13–15]. This lateral inhibition ensures that only some of the cells of the prosensory domain retain the transcription factor *Atoh1* [16,17]. *Atoh1* is both necessary and sufficient for HC differentiation [18]. In contrast to the apical to

basal wave of cell cycle exit of the prosensory domain, the wave of differentiation occurs basally at E14.5 extending apically at E17.5 [19].

In addition to the above, fibroblast growth factor (FGF) signalling has also been shown to be important in the development of the cochlear HC. Conditional deletion of *Fgf receptor (Fgfr) 1*, results in the loss of HCs [20]. This phenotype is observed to a lesser extent, when the proposed ligand for FGFR1, *Fgf20*, is deleted [21]. *Ex vivo* explant studies suggest that FGF signalling enhances Notch-Jag signalling after sensory patch induction [22]. However the *in vivo* significance of these observations and how they lead to the *Fgfr1* deletion phenotype are not clear.

Fgf ligand binding causes the dimerization and activation of the canonical receptor tyrosine kinase [23]. Activation, generally by phosphorylation of particular tyrosine residues in the intracellular domain of the Fgf receptor, results in recruitment of adaptor proteins that are essential for the intracellular response to the extracellular signal. Each group of phosphorylated residues mediate distinct functions, for example phosphorylation of tyrosine 766 in FGFR1 serves as a potential binding site for phospholipase C- γ (PLC γ) [24]. Other adaptor proteins include Fgf Receptor Substrate (Frs) 2 or 3 (collectively termed Frs2/3) [25,26]. Frs2/3 recruitment and activation leads to the stimulation of multiple FGFR-dependent signaling pathways such as Ras/MAP kinase pathway, and the phosphatidylinositol-3-kinase (PI3K) pathway [27]. Studies into a mouse allele in which the Frs2/3 interaction motif has been deleted, reveal that Frs2/3 recruitment mediates aspects of FGFR1

Author Summary

The ability of our brain to perceive sound depends on its conversion into electrical impulses within the cochlea of the inner ear. The cochlea has dedicated specialized cells, called inner ear hair cells, which register sound energy. Environmental effects, genetic disorders or just the passage of time can damage these cells, and the damage impairs our ability to hear. If we could understand how these cells develop, we might be able to exploit this knowledge to generate new hair cells. In this study we address an old problem: how do signals from the fibroblast growth factor (FGF) family control hair cell number? We used mice in which one of the receptors for FGF (Fgfr1) is mutated and found that the expression of a stem cell protein, Sox2 is not maintained. Sox2 generally acts to keep precursors in the cochlea in a pre-hair cell state. However, in mutant mice Sox2 expression is transient, diminishing the ability of precursors to commit to a hair cell fate. These findings suggest that it may be possible to amplify the number of hair cell progenitors in culture by tuning FGF activity, providing a route to replace damaged inner ear hair cells.

signalling [28]. However, the necessity of these pathways in inner ear development had not been investigated.

In this study, we found that FGFR1 signalling through Frs2/3 is necessary for prosensory formation. Even in the absence of FGFR1-Frs2/3 signalling, the prosensory domain becomes post-mitotic, however the expression of prosensory markers is impaired. This results in fewer sensory precursors, giving rise to a reduction in HC numbers. We also found that the expression of Sox2 is transient, suggesting that the strength and duration of Sox2 expression, under the direct or indirect control of FGF-mediated MAP kinase activation, commits progenitors to sensory cell differentiation.

Results

FGFR1 signalling through Frs2/3 recruitment is required for normal cochlear hair cell development

To determine gross morphology, the inner ear from *Six1enh21-Cre::Fgfr1^{lox/lox}* and *Fgfr1^{ΔFrs/ΔFrs}* at E14.5 were examined first by paint-filling [29]. The cochlear duct of the conditional mutant (*Six1enh21-Cre::Fgfr1^{lox/lox}*) was shorter than control (Figure 1A and B). *Fgfr1^{ΔFrs/ΔFrs}* also exhibited a truncated cochlear duct although the phenotype was milder than that of the conditional mutant (Figure 1C). No significant difference in the formation of vestibular components was observed.

A requirement for FGFR1 function in cochlear HC development had been previously shown [20], however the mechanisms used remained unknown. We asked when FGFR1 signalling was acting during HC development, by exploiting the difference in the timing activation of of two different Cre driver lines. To first verify Cre activity, we crossed these lines with a *Rosa26-flox-STOP-flox-EYFP* reporter, in which the expression of EYFP is initiated after the Cre-mediated excision of the STOP, transcription terminator sequence. *Six1enh21-Cre* activity can be detected as early as E9.5 specifically in whole otic epithelium (Figure 2A–C and G). In contrast, *Emx2-Cre* activity cannot be detected at E9.5, but is active at E12.5, with EYFP labelled in the almost all putative sensory organs except three semicircular ampullae (Figure 2D–G and data not shown). Quantitative PCR for the deleted portion of *Fgfr1* confirmed the temporal activity of the two Cre lines (Figure 2H). *Fgfr1* levels in the cochlear rudiment were reduced to approximately

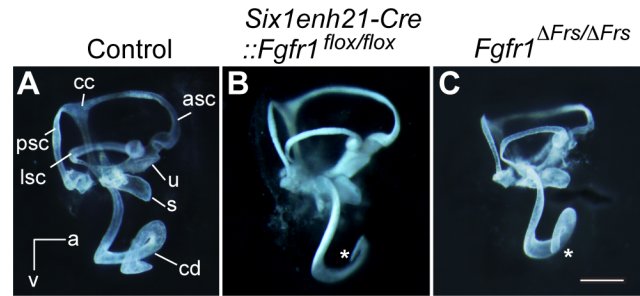


Figure 1. Inner ear development is disrupted in *Fgfr1* mutants. (A) The morphology of the inner ear was revealed by the injection of white paint. Control inner ears show a typical morphology consisting of 3 semi-circular canals and the spiral cochlear duct that is 1.5 turns long. (B) The inner ear of *Six1enh21-Cre::Fgfr1^{lox/lox}* exhibits only 1 turn of the cochlear duct (asterisk). Vestibular components are unaffected. (C) *Fgfr1^{ΔFrs/ΔFrs}* inner ear shows milder cochlear phenotype than that of *Six1enh21-Cre::Fgfr1^{lox/lox}* with a slightly shortened cochlear duct (asterisk). cd, cochlear duct; u, utricle; s, saccule; psc, posterior semicircular canal; asc, anterior semicircular canal; lsc, lateral semicircular canal; cc, common crus; a, anterior; v, ventral. doi:10.1371/journal.pgen.1004118.g001

20% of normal in *Six1enh21-Cre::Fgfr1^{lox/lox}* from E10.5. In contrast, *Fgfr1* levels in *Emx2-Cre::Fgfr1^{lox/lox}* cochleae were close to wild-type levels at E10.5, falling to 60% at E12.5 and 20% by E14.5. We thus used these lines to examine the cochlear phenotypes when *Fgfr1* deletion occurred at around E9.5 to 10.5 (using *Six1enh21-Cre*) or at around E12.5 (using *Emx2-Cre*).

To investigate HC phenotype, whole-mount cochlear samples from E18.5 mice were dissected and immunostained for Myo7a. Control, wild-type, cochleae showed the typical arrangement of three rows of OHCs and one row of IHCs along the entire length of the cochlea (Figure 3A, B). In *Six1enh21-Cre::Fgfr1^{lox/lox}* the arrangement of HCs was altered, with those in the apical third of the cochlea more severely affected (Figure 3C–E). Here the rows of HCs were discontinuous, and arranged in islands. Typically, OHCs were missing, although isolated OHCs could be found basally. The cochlear phenotype of *Emx2-Cre::Fgfr1^{lox/lox}* inner ears was milder (Figure 3F–H). Basally, OHC loss was less pronounced with the outer-most row most severely affected (Figure 3F). Further apically, the HC row became discontinuous, and islands that were present were made up of IHCs and OHCs, with occasional additional IHCs observed (Figure 3G). HCs were more sparsely distributed in the apical-most part of the cochlea (Figure 3H).

We next addressed the downstream pathway employed by FGFR1 during cochlear HC formation using two alleles of *Fgfr1*, *Fgfr1^{ΔFrs/ΔFrs}* and *Fgfr1^{Y766F/Y766F}*. Y766F carries a point mutation converting a tyrosine at position 766 to a phenylalanine, rendering it resistant to phosphorylation. This has been postulated to result in a failure of PLC γ phosphorylation and thus its activation [30]. The cochlear HC phenotype of *Fgfr1^{ΔFrs/ΔFrs}* inner ears closely resembled that of *Six1enh21-Cre::Fgfr1^{lox/lox}*, showing the severe OHC loss apically and the islands of HCs (Figure 3I–K). In contrast, surface preparations from the inner ear of *Fgfr1^{Y766F/Y766F}* showed that cochlear HCs were normal (Figure 3L). The correspondence of the HC phenotypes was confirmed after quantifying the number of cochlear HCs, and also compared to the previously published *Foxg1-Cre::Fgfr1^{lox/lox}* [20]. The total number of HCs per cochlea averaged 2494 ± 160 ($n = 4$) in wild-type controls. There were 201 ± 26 ($n = 4$) HCs in *Six1enh21-Cre::Fgfr1^{lox/lox}* inner ears, 218 ± 44 in *Foxg1-Cre::Fgfr1^{lox/lox}* cochlea ($n = 4$), 728 ± 274 ($n = 6$) in *Emx2-Cre::Fgfr1^{lox/lox}*, 420 ± 60 ($n = 5$) in *Fgfr1^{ΔFrs/ΔFrs}*, and 2532 ± 23 ($n = 6$) in *Fgfr1^{Y766F/Y766F}* (mean \pm SD,

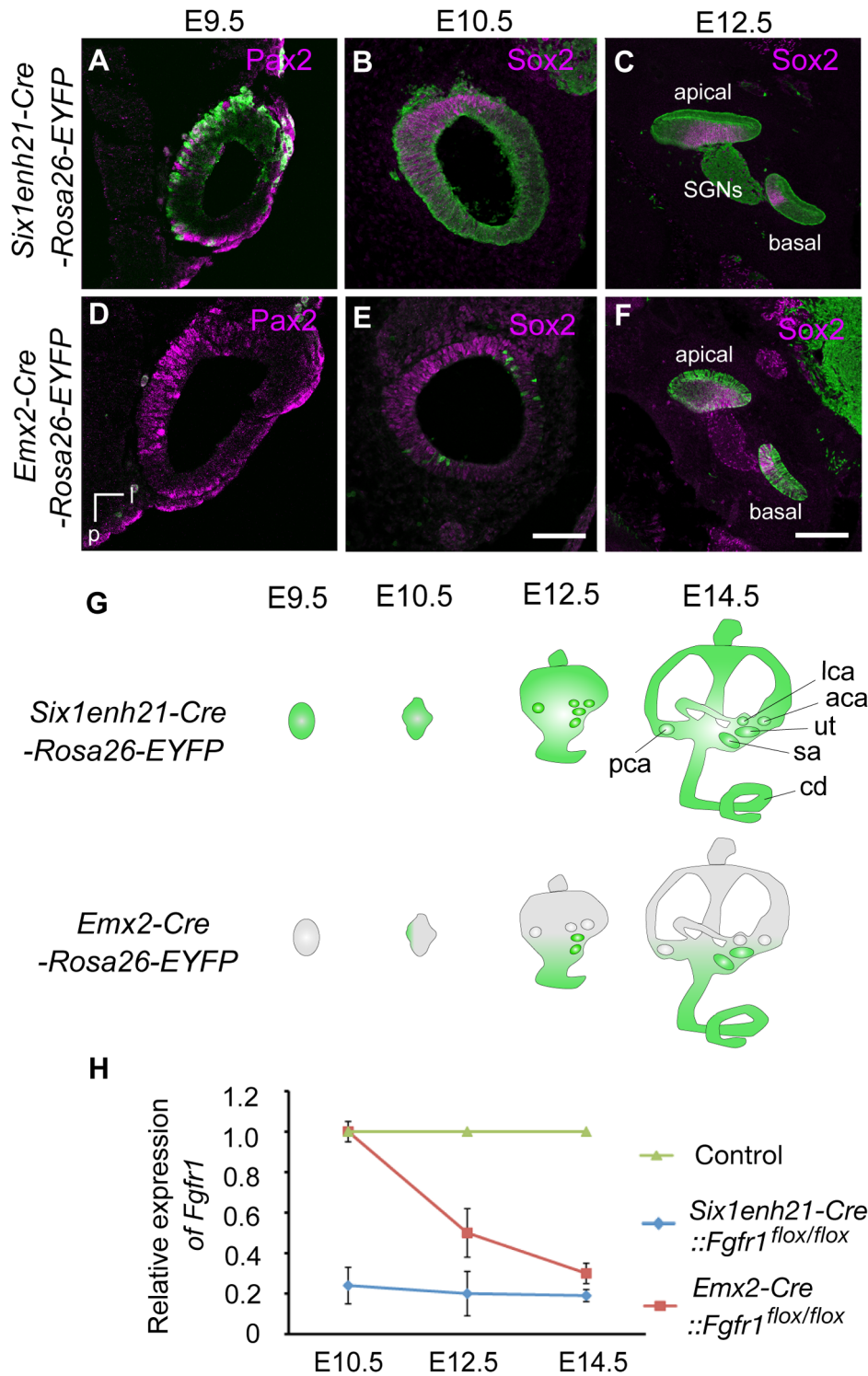


Figure 2. Spatio-temporal activity of conditional Cre drivers. (A–F) EYFP expression under control of *Six1enh21-Cre* or *Emx2-Cre* at E9.5, E10.5, and E12.5. *Six1enh21-Cre*-mediated EYFP expression is detectable in a majority of otic cells, marked by Pax2, by E9.5 (A). All of Sox2 expressing otic cells colocalize with Cre-mediated EYFP by E10.5 (B). The early activity results in detectable EYFP expression in the spiral ganglion cells as well as epithelial cells that include sensory competent cells marked by Sox2 at E12.5 (C). In contrast, very few *Emx2-Cre*-mediated EYFP expressing cells can be detected at E9.5 (D). The onset of *Emx2-Cre* activity in the inner ear is around E10.5 in the lateral wall of otocyst (E), and becomes uniform by E12.5 throughout the cochlear duct (F). (G) Schematic illustration depicting spatio-temporal activity (green) of each Cre driver during inner ear development. (H) RT-PCR analysis showing temporal deletion of *Fgfr1* by two Cre lines. Mean \pm SD are shown. cd, cochlear duct; u, utricle; s, saccule; psc, posterior semicircular canal; asc, anterior semicircular canal; lsc, lateral semicircular canal; l, lateral; v, ventral; p, posterior; SGNs, spiral ganglion neurons. Scale bars: A, B, D, and E, 75 μ m (in E); C and F, 150 μ m (in F). doi:10.1371/journal.pgen.1004118.g002

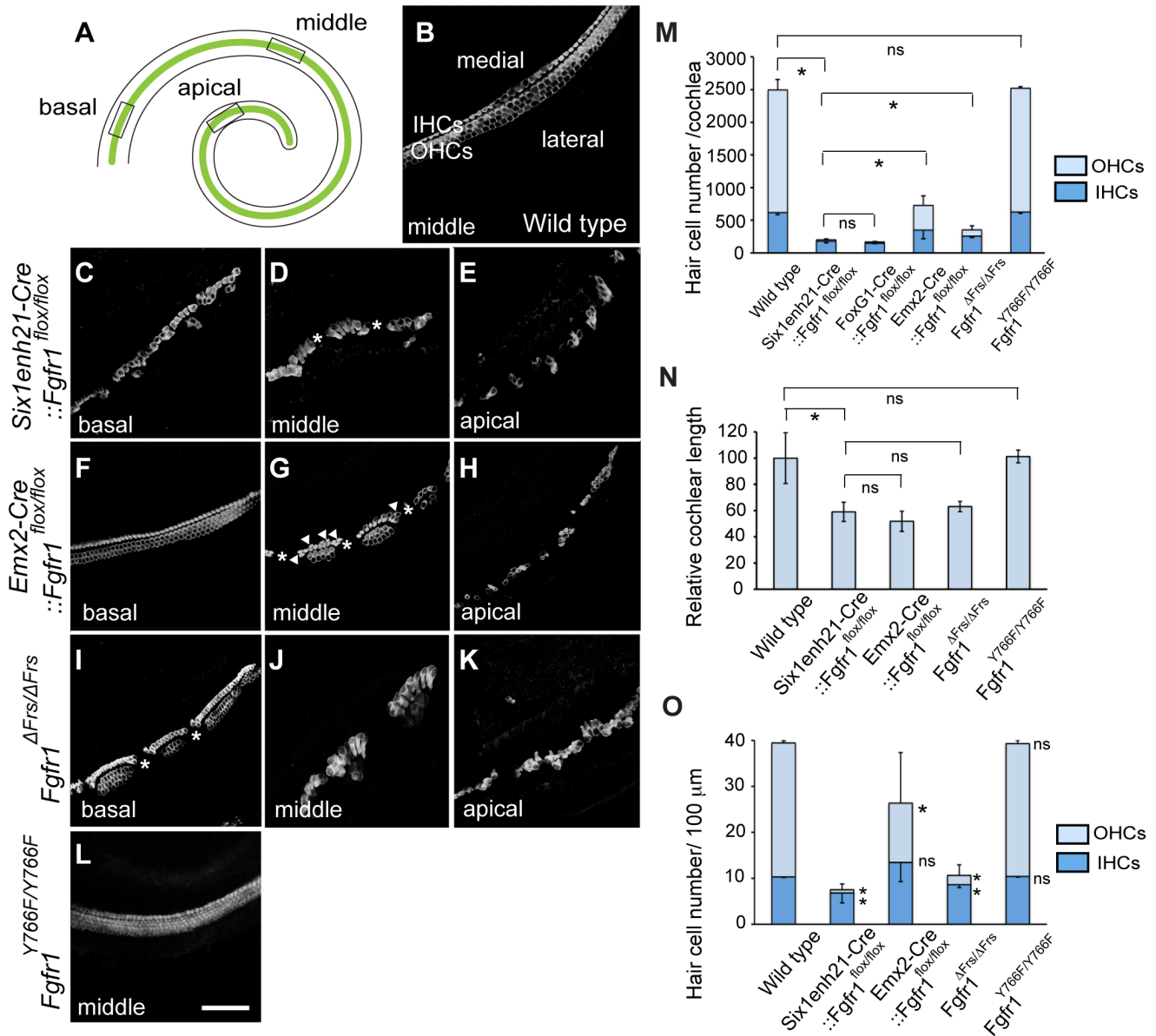


Figure 3. Cochlear hair cells are reduced in *Fgfr1* mutants. (A) Schematic of whole mount view of neonatal cochlear duct. HCs are arranged along the entire length of cochlear duct. (B) Magnified view of wild type cochlear duct labeled with anti-Myo7a antibody. Highly ordered array of three rows of OHCs and one row of IHCs are observed. (C–E) HCs are disrupted in *Six1enh21-Cre::Fgfr1^{flox/flox}* cochlea. Basally, few OHCs are visible (C). In the middle, there are small gaps in the remaining IHCs (asterix) (D). Apically, sparsely distributed HCs are observed (E). (F–H) *Emx2-Cre::Fgfr1^{flox/flox}* mice show a less severe phenotype. Basally, IHCs and OHCs form, although only two rows of OHCs form (F). In the middle region, islands of HCs form between gaps (asterix). Additional IHCs are occasionally observed (arrowheads) (G). Apically, islands are sparse (H). (I–K) *Fgfr1^{ΔFrs/ΔFrs}* cochlea shows a less severe phenotype than that of *Six1enh21-Cre::Fgfr1^{flox/flox}* cochlea, but more severe phenotype than *Emx2-Cre::Fgfr1^{flox/flox}* cochlea. Basally, some IHCs and OHCs form, although frequently arranged in islands, punctuated by gaps (asterix). (L) The number of rows of HCs and their patterning are unaffected in *Fgfr1^{Y766F/Y766F}* mutant cochlea. (M) Stacked graph comparing the number of cochlear IHCs and OHCs amongst different *Fgfr1* mutants. Sum of each number represents total HC number. Statistic significance is shown for total HC number. Error bars (mean \pm SD) represent variation in each HC type. (N) Graph showing relative length of cochlear duct at E18.5. Cochlear length is decreased by approximately 40–50% in all *Fgfr1* mutants except *Fgfr1^{Y766F/Y766F}*. (O) Number of IHCs and OHCs are counted and normalized to 100 μ m from different *Fgfr1* mutants. Sum of each number represents total HC number per 100 μ m. Statistic significance is shown for each HC type, compared with the number of HCs from wild type. Error bars (mean \pm SD) represent variation in each HC type. * $p < 0.05$. ns, not significant. Scale bar: C–L; 50 μ m (in L). doi:10.1371/journal.pgen.1004118.g003

respectively) (Figure 3M). The significant difference was also determined when comparing *Six1enh21-Cre::Fgfr1^{flox/flox}* and *Emx2-Cre::Fgfr1^{flox/flox}* cochleae ($p < 0.05$). Given the differences in the timing of the two Cre drivers (Figure 2), these results suggest that FGFR1 signalling commences prior to E12.5.

Next we counted the number of IHCs and OHCs (Figure 3M). By comparisons with control cochlea (1876 ± 160), OHC loss were evident in *Six1enh21-Cre::Fgfr1^{flox/flox}* (22 ± 14 , decreased by 99%), *Emx2-Cre::Fgfr1^{flox/flox}* (379 ± 144 , decreased by 80%), and *Fgfr1^{ΔFrs/ΔFrs}* (93 ± 77 , decreased by 95%), but not in *Fgfr1^{Y766F/Y766F}*

(1894±24). With the exception of *Fgfr1*^{E766F/1766F} mutants (626±19), the number of IHCs were also reduced in FGFR1 signaling mutants; *Six1enh21-Cre::Fgfr1*^{lox/lox} (179±25, decreased by 72%), *Emx2-Cre::Fgfr1*^{lox/lox} (349±130, decreased by 44%), and *Fgfr1*^{ΔFrs/ΔFrs} (259±61, decreased by 58%), compared with wild type control (618±31) ($p < 0.05$). In addition, cochlear length was decreased by 41% in *Six1enh21-Cre::Fgfr1*^{lox/lox}, by 49% in *Emx2-Cre::Fgfr1*^{lox/lox}, and by 37% in *Fgfr1*^{ΔFrs/ΔFrs} mutants, respectively (Figure 3N). To exclude the influence of cochlear length on total HC number, we counted the number of each HC type normalized to 100 μm length (Figure 3O). IHCs were decreased ($p < 0.05$) by 33% in *Six1enh21-Cre::Fgfr1*^{lox/lox} (6.8±2.1), by 17% in *Fgfr1*^{ΔFrs/ΔFrs} (8±0.1) of wild type levels (10.3±0.1). However, normalized number of IHCs was statistically the same in *Emx2-Cre::Fgfr1*^{lox/lox} (13.4±4.1) and wild type (10.3±0.1). In contrast, OHC number per 100 μm was decreased by 98% in *Six1enh21-Cre::Fgfr1*^{lox/lox} (0.7±1.2), by 56% in *Emx2-Cre::Fgfr1*^{lox/lox} (12.8±11.1), and by 87% in *Fgfr1*^{ΔFrs/ΔFrs} (2.0±2.2) when compared to wild type levels (29.1±0.4). These findings suggested that FGFR1-Frs2/3 activity was required for OHC development from E10.5, whereas FGFR1-Frs2/3 activity was only required for IHC development prior to E12.5. Taken together, these results demonstrate that signalling via Frs2/3 recruitment is necessary for FGFR1 activity during the formation of the cochlear HCs.

In addition to the cochlear HC phenotype, we analyzed the number of HCs in one of the vestibular sense organs, the utricle dissected from E16.5 mice. While utricular HCs number was comparable between *Six1enh21-Cre::Fgfr1*^{lox/+} (577±21, $n = 3$) and *Six1enh21-Cre::Fgfr1*^{lox/lox} (550±10, $n = 4$) (Figure 4A, B), HC number was significantly decreased ($p < 0.05$) in *Fgfr1*^{ΔFrs/ΔFrs} mutants (473±57, $n = 6$), by comparison with *Fgfr1*^{ΔFrs/+} control (718±81, $n = 4$) (Figure 4C, D). As this mutant is non-conditional, it may suggest that FGFR1 signalling outside of the inner ear epithelium plays a role in vestibular HC formation.

Support cell development is perturbed in the absence of Frs2/3-mediated FGFR1 signalling

The decision by sensory precursors to generate either HCs or SCs is controlled by Notch-Delta cell-cell signalling [5,13–15]. Therefore, one possible mechanism of FGFR1 action is in modifying the action of Notch and Delta in this choice. We thus investigated whether SC formation was disrupted in the absence of Frs2/3-mediated FGFR1 signalling. We crossed *Fgfr1*^{ΔFrs/ΔFrs} onto an *Atoh1-GFP* reporter line to reveal HCs. At E18.5, Prox1 is strongly expressed in the Deiter's cells and in the pillar cells [31]. In the control, *Fgfr1*^{ΔFrs/+} cochlea, Prox1-labeled 5 rows of cells (Figure 5A). In mutant *Fgfr1*^{ΔFrs/ΔFrs} cochlea, only two to three rows of Prox1-labelled cells were detected and were confined within sensory islands (Figure 5B). In whole mount view of *Fgfr1*^{ΔFrs/+} cochlea, p75 expression was apparent in the inner pillar cells that are found along the length of the cochlear duct (Figure 5C). In *Fgfr1*^{ΔFrs/ΔFrs} cochlea, p75 staining was only found in the sensory cell islands highlighted by Atoh1-GFP and not found in the intervening spaces (Figure 5D). Within severely affected region, the row of p75-positive cells was mostly present lateral to the one row of HCs, suggesting that these islands were exclusively IHCs.

The other SC marker at this stage, Sox2, was also only found within the sensory islands (Figure 5E and F). Section analysis revealed that Sox2 is expressed in SCs, in both control organ of Corti (Figure 5G) and in sections taken through the level of the islands in *Fgfr1*^{ΔFrs/ΔFrs} cochlea (Figure 5H). In sections taken through the gaps in between the islands, we could only detect weak Sox2 expression in the Kölliker's organ, a region medial to lateral

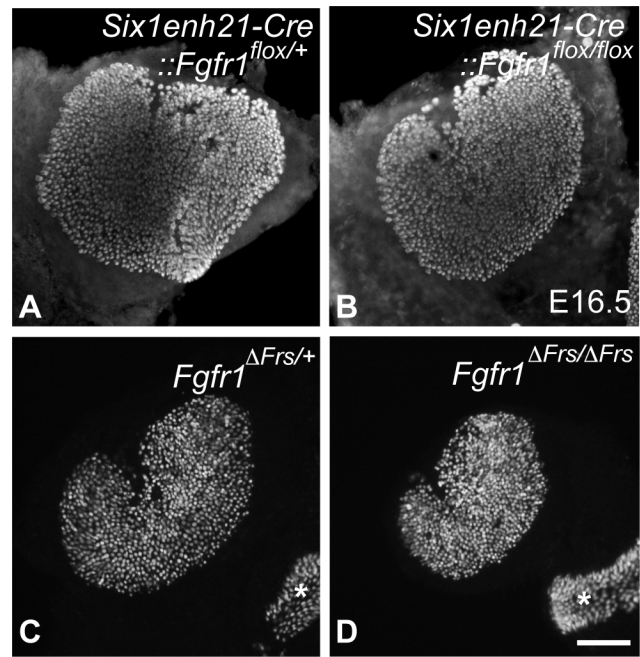


Figure 4. Disruption of FGFR1-Frs2/3 pathway decreases the number of vestibular hair cells. (A, B) No change in HC number was detected between E16.5 *Six1enh21-Cre::Fgfr1*^{lox/+} (A) and *Six1enh21-Cre::Fgfr1*^{lox/lox} utricles (B) labeled with anti-Myo7a antibody. (C, D) Fewer HCs were observed in the utricle of E16.5 *Fgfr1*^{ΔFrs/ΔFrs} mutants (D) than *Fgfr1*^{ΔFrs/+} control (C). Ampullary HCs are also included (asterisks). Scale bar: A–D; 200 μm (in D). doi:10.1371/journal.pgen.1004118.g004

compartment (Figure 5I). Combined, these results suggest that the FGFR1-Frs2/3 signalling axis also affects the formation of SCs, and is thus acting upstream of HC/SC decision mediated by Notch-Delta signalling.

FGFR1/Frs2/3 interaction is not essential for FGFR1-mediated cell cycle regulation during inner ear development

Precursors of auditory HCs and SCs form from a domain known as the prosensory domain [1]. This region emerges from within the Sox2-positive sensory patch between E12.5 and E14.5, depending on the exact position within the cochlea. It is initially characterised by the cessation of mitosis, forming the zone of non-proliferating cells (ZNPC), as well as the expression of a cell cycle inhibitor, p27^{Kip1}. Subsequently, the ZNPC expresses specific markers of the prosensory domain such as Hey2 and Hes5. It had been previously shown that a conditional deletion of *Fgfr1* regulates proliferation in the cochlea [20]. We thus asked if cell cycle regulation within the cochlea was mediated by FGFR1-mediated Frs2/3 activity.

We first asked if *Six1enh21-Cre::Fgfr1*^{lox/lox} mutants used in this study recapitulated the reported cell cycle deficit shown previously in *FoxG1-Cre::Fgfr1*^{lox/lox} [20]. Prosensory domain progenitors become post-mitotic commencing at the apex at E12.5 and ending at the base at E14.5. Cell cycle exit correlates with the expression of p27^{Kip1}, as was observed in whole mount preparations of control heterozygous cochlea stained for p27^{Kip1} and BrdU (Figure 6A and B). Consistent with previous observations, no cell cycle defect was detected in *Six1enh21-Cre::Fgfr1*^{lox/lox} mutant at E10.5 (data not shown) [20]. However, a reduction in cell proliferation within the epithelial cells of the cochlea was detected

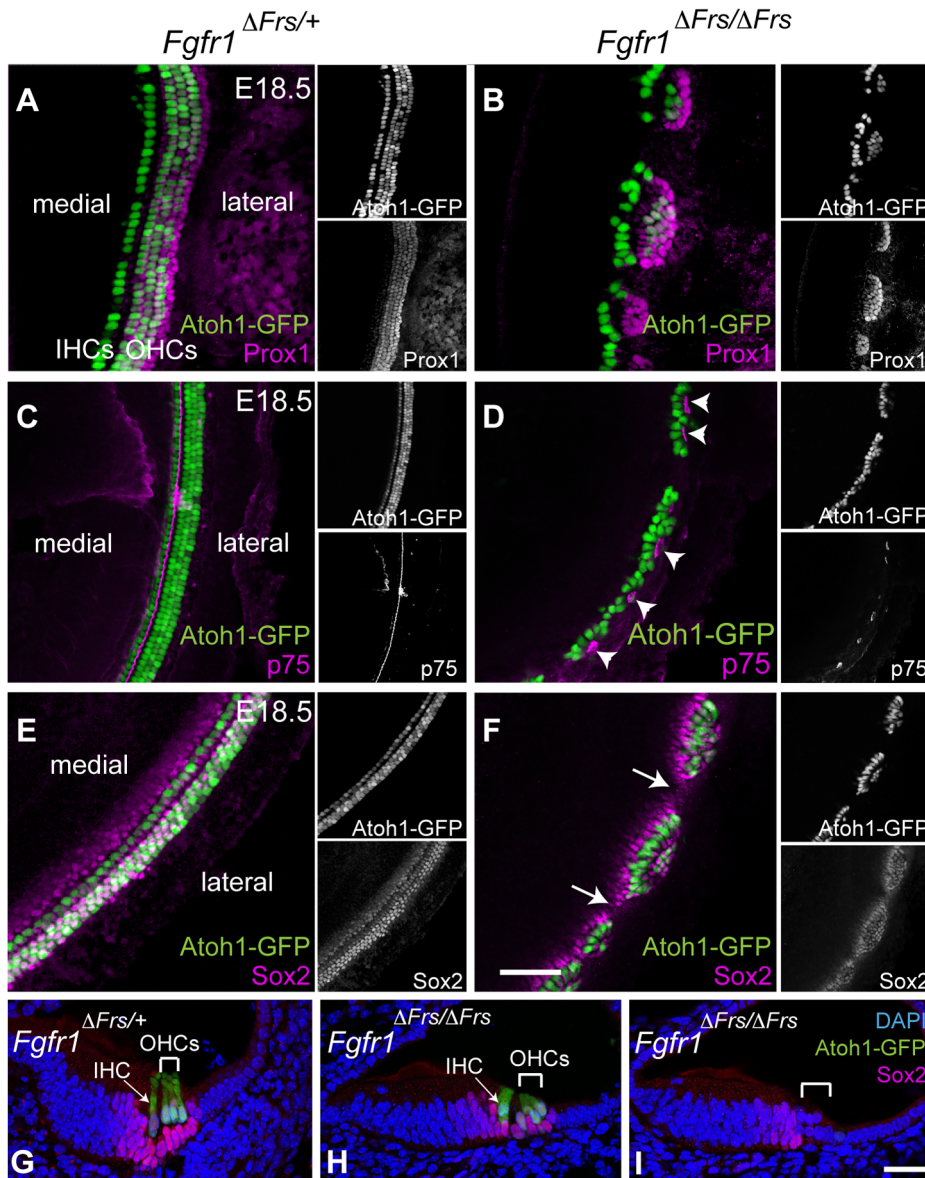


Figure 5. Disruption of FGFR1-Frs2/3 pathway decreases the number of support cells. (A) Prox1 immunostaining (magenta) marks cochlear SCs; the pillar cells and Deiter's cells in heterozygous *Fgfr1*^{ΔFrs/+} cochlea at E18.5. This line also expresses GFP under the control of the Atoh1 enhancer marking HCs (green). (B) In mutant *Fgfr1*^{ΔFrs/ΔFrs} cochlea, HCs form Atoh1-GFP-positive sensory islands. Prox1-positive SCs are not detected in the space between these islands. (C) In *Fgfr1*^{ΔFrs/+} control cochlea at E18.5, expression of p75 (magenta), a marker for pillar cells, marks adjacent to the IHCs. (D) p75 is observed in patches in mutant *Fgfr1*^{ΔFrs/ΔFrs} cochlea (arrowheads), and it is not detected in the gaps between islands. Note that most Atoh1-GFP-positive HCs are located medial to p75-expressing pillar cells. (E) In heterozygous *Fgfr1*^{ΔFrs/+} cochlea at E18.5, Sox2 (magenta) marks SCs arranged in rows coincident with Atoh1-GFP-positive HCs. (F) In mutant *Fgfr1*^{ΔFrs/ΔFrs} cochlea, Sox2 expression extends beyond the sensory islands, but is not detected in the gaps (arrows). (G) Transverse section view of organ of Corti from E18.5 *Fgfr1*^{ΔFrs/+} expressing GFP under the control of the Atoh1 enhancer, labeled with Sox2. One IHC (arrow) and three OHCs (bracket) are observed. Sox2 is expressed in surrounding SCs, including Deiter's cells, pillar cells, inner phalangeal cell, and Kölliker's organ. (H) Cross section of a sensory island from E18.5 mutant *Fgfr1*^{ΔFrs/ΔFrs} cochlea. Here, one IHC (arrow) and two OHCs (bracket) are detected. Sox2 expression is detected in surrounding SCs. (I) Cross section of a gap intervening sensory islands from mutant *Fgfr1*^{ΔFrs/ΔFrs} cochlea. No HCs are detected and Sox2 is only detectable in Kölliker's organ, but not in lateral compartment (bracket). Nuclei are visualized by DAPI. Scale bars: A–F, 50 μm (in F); G–I, 30 μm (in I). doi:10.1371/journal.pgen.1004118.g005

in *Six1enh21-Cre::Fgfr1*^{flox/flox} mice at E12.5 (Figure 6C). This phenotype was more prominent in Kölliker's organ at E13.5 and E14.5. Surprisingly, and despite the proper formation of the ZNPC, p27^{Kip1} was down-regulated in *Six1enh21-Cre::Fgfr1*^{flox/flox} cochlea at E13.5 and E14.5 when compared to controls (Figure 6D). Quantification of BrdU-labelled cells showed far fewer proliferating cells in E12.5 nascent cochlear duct of

Six1enh21-Cre::Fgfr1^{flox/flox} (14±8; n=5 compared with 41±8; n=4 in wild type controls) and E14.5 Kölliker's organ (2±2; n=5 compared with 21±4; n=5 in wild type controls) (*p*<0.05) (Figure 6G).

We next investigated proliferation in *Fgfr1*^{ΔFrs/ΔFrs} cochlea. *Fgfr1*^{ΔFrs/ΔFrs} mutant cochlea still exhibited down-regulation of p27^{Kip1} throughout cochlear duct (Figure 6F). However in

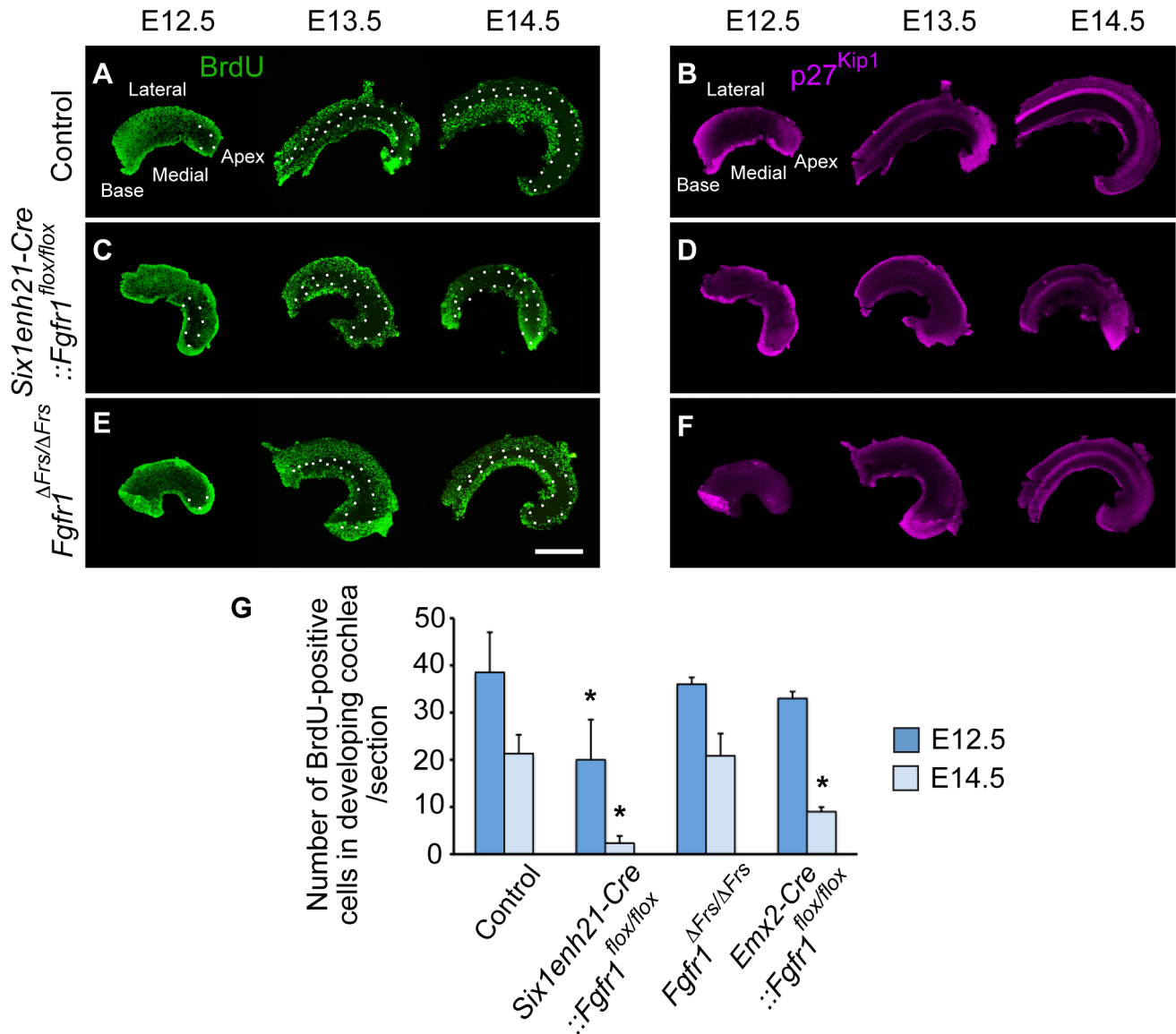


Figure 6. FGFR1-mediated cell proliferation is not mediated by Frs2/3 interaction. Cochlear whole mounts from controls (A, B), *Six1enh21-Cre::Fgfr1^{flox/flox}* (C, D) and *Fgfr1^{ΔFrs/ΔFrs}* (E, F) were assessed for incorporation of BrdU injected 2 hours before sacrifice (A, C, E) and the expression of p27^{Kip1} (B, D, F) at E12.5, E13.5, and E14.5. (A) The pattern of BrdU uptake indicates that the ZNPC (circled by dotted line) is first apparent at E12.5 in the apex of control cochlea and extends basally by E14.5 in control cochlea. At E13.5 and E14.5, proliferation in Kölliker's organ medial to the ZNPC is apparent. (B) p27^{Kip1} protein expression is co-incident with the ZNPC in control cochlea at E12.5 to E14.5. (C) The ZNPC was still detected in *Six1enh21-Cre::Fgfr1^{flox/flox}* cochlea apically at E12.5, extending basally by E14.5. Reduced BrdU uptake was noted in Kölliker's organ. (D) p27^{Kip1} protein expression in apical region was normal at E12.5, but reduced in *Six1enh21-Cre::Fgfr1^{flox/flox}* cochlea at E13.5 and E14.5. (E) BrdU immunostaining revealed that the ZNPC also formed normally in *Fgfr1^{ΔFrs/ΔFrs}* cochlea from E12.5. However, robust proliferation was noted in Kölliker's organ at E13.5 and E14.5. (F) p27^{Kip1} protein expression in apical region was normal at E12.5, but reduced in *Fgfr1^{ΔFrs/ΔFrs}* cochlea at E13.5 and E14.5, compared to control. (G) Graph showing the number of BrdU-positive cells in the cochlea at E12.5 and in Kölliker's organ at E14.5. BrdU-labelled cells were reduced in *Six1enh21-Cre::Fgfr1^{flox/flox}* cochleae at both E12.5 and E14.5. In *Emx2-Cre::Fgfr1^{flox/flox}* mutant cochlea, there was no significant reduction in proliferation at E12.5, but a reduction in BrdU uptake was noted in Kölliker's organ at E14.5. No difference was detected between control and *Fgfr1^{ΔFrs/ΔFrs}* cochlea. * $p < 0.05$. Scale bar: 75 μ m. doi:10.1371/journal.pgen.1004118.g006

contrast to *Six1enh21-Cre::Fgfr1^{flox/flox}* mutant cochlea, BrdU-positive cells were observed in Kölliker's organ of *Fgfr1^{ΔFrs/ΔFrs}* mutant (Figure 6E). Comparable number of BrdU-positive cells were detected in *Fgfr1^{ΔFrs/ΔFrs}* at both stages (36 ± 8 ; $n = 4$ at E12.5, and 21 ± 5 ; $n = 5$ at E14.5) ($p < 0.05$) (Figure 6G). We also quantified the number of BrdU-positive cells in *Emx2-Cre::Fgfr1^{flox/flox}* cochleae. Reduced proliferation was only detected at E14.5 and was milder

than that observed for *Six1enh21-Cre::Fgfr1^{flox/flox}* (39 ± 1 ; $n = 4$ at E12.5, and 9 ± 1 ; $n = 4$ at E14.5). These results indicate that Frs2/3 recruitment does not mediate FGFR1-induced cell proliferation in Kölliker's organ during inner ear development. Furthermore, these results showed that FGFR1-Frs2/3 signaling is not necessary for the formation of the ZNPC, but is required for p27^{Kip1} expression.

Formation of the prosensory domain is disrupted by lack of FGFR1-Frs2/3 signalling

The down-regulation of $p27^{Kip1}$ expression in the prosensory domain indicated that even though prosensory precursors had become post-mitotic, a marker of the prosensory domain was not correctly expressed. Section analysis revealed that as well as $p27^{Kip1}$ (Figure 7A–C), the prosensory domain marker *Hey2* was also reduced in cochlea from both *Six1enh21-Cre::Fgfr1^{lox/lox}* and *Fgfr1^{ΔFrs/ΔFrs}* mutants (Figure 7D–F). We confirmed the down-regulation of $p27^{Kip1}$ and *Hey2*, as well as two other prosensory markers, *Hes5* and *Atoh1*, by quantitative PCR (Figure 7P). The down-regulation of prosensory domain markers was significantly milder in *Emx2-Cre::Fgfr1^{lox/lox}* cochleae than in either *Six1enh21-Cre::Fgfr1^{lox/lox}* or *Fgfr1^{ΔFrs/ΔFrs}* mutants (Figure 7P).

As well as the prosensory domain, the Sox2-positive sensory patch also forms Kölliker's organ and the outer sulcus. We thus asked if *Fgfr1* mutation also affected these structures. Cells in Kölliker's organ normally express *Fgf10* and *Jag1*. In both *Six1enh21-Cre::Fgfr1^{lox/lox}* and *Fgfr1^{ΔFrs/ΔFrs}* mutants, the spatial expression of *Jag1* (Figure 7G–I) and *Fgf10* (Figure 7J–L) was unchanged. However, quantitative PCR revealed a down-regulation of *Fgf10* expression, although *Jag1* did not show any significant difference (Figure 7P). The spatial pattern of *Bmp4*, a marker for the outer sulcus located lateral to prosensory domain, was also unchanged in *Six1enh21-Cre::Fgfr1^{lox/lox}* and *Fgfr1^{ΔFrs/ΔFrs}* mutants (Figure 7M–O). Quantitation revealed up-regulation of *Bmp4* only in *Six1enh21-Cre::Fgfr1^{lox/lox}* mutant but not in *Fgfr1^{ΔFrs/ΔFrs}* (Figure 7P). These results indicate that although cell cycle exit, an aspect of prosensory domain induction, occurred normally, the induction of genes marking the prosensory domain is impaired in the absence of Frs2/3-mediated FGFR1 signalling. This signalling also contributes to the up-regulation of *Fgf10* in Kölliker's organ. However, FGFR1 signalling independently of Frs2/3 recruitment, may negatively regulate *Bmp4* expression in the outer sulcus.

FGFR1 is necessary for Sox2 maintenance during sensory patch formation

The expression of Sox2 in the sensory patch is known to be critical in the formation of prosensory domain and subsequent HC formation; mutation or reduction in Sox2 expression affects their development in a dose-dependant fashion [2]. Furthermore, FGF signalling has been shown to be sufficient for Sox2 expression [22]. We thus hypothesised that the HC phenotype observed in *Fgfr1* mutants were, in part, due to alterations in Sox2 expression. Initially, Sox2 is expressed in the neuronal and sensory precursors in the otocyst at E10.5. Between E12.5 to E14.5, Sox2 expression in the cochlear duct is detected in the thickened epithelial cells that mark the site of the prosensory domain [32]. By E18.5, Sox2 is confined to the SCs of the organ of Corti [4].

Sox2 was initially expressed at comparable levels between control, heterozygous, inner ears and *Six1enh21-Cre::Fgfr1^{lox/lox}* mutants at E10.5 (Figure 8A and B). By E11.5, expression in *Six1enh21-Cre::Fgfr1^{lox/lox}* inner ears was decreased (Figure 8D), although in *Fgfr1^{ΔFrs/ΔFrs}* expression levels were equivalent to those in control inner ears (Figure 8C and E). By E12.5, decreased expression of Sox2 in the cochlea of both *Fgfr1* mutant lines was apparent (Figure 8F–H), although Sox2 expression in the saccule was unchanged. To quantify this decrease, we measured Sox2 protein levels in E12.5 mouse cochlea. Levels were reduced by approximately 78% in *Six1enh21-Cre::Fgfr1^{lox/lox}* to the levels found in *Six1enh21-Cre::Fgfr1^{lox/+}*, while a 55% decrease was observed in *Fgfr1^{ΔFrs/ΔFrs}* when compared to heterozygous controls (Figure 9A). This down-regulation was confirmed by immunostaining whole

cochleae with Sox2 antibody (Figure 9B and C). To exclude the possibility that the early Sox2 down-regulation occurred due to accelerated prosensory domain development, we used BrdU uptake to indicate its formation. At E12.5, even though Sox2 is down-regulated in the cochlear rudiment of *Six1enh21-Cre::Fgfr1^{lox/lox}*, BrdU-positive cells can still be detected (Figure 9D and E), indicating that Sox2 down-regulation occurred prior to prosensory domain formation. Furthermore, the down-regulation is not a result of cell survival: No difference in cell death was observed between controls and *Six1enh21-Cre::Fgfr1^{lox/lox}* cochleae using an antibody against activated caspase-3 to detect apoptotic cells (data not shown).

At E14.5, the onset of sensory cell differentiation, Sox2 is expressed robustly in the prosensory domain (Figure 10A). *Six1enh21-Cre::Fgfr1^{lox/lox}* (Figure 10B) and *Fgfr1^{ΔFrs/ΔFrs}* cochleae (Figure 10C) showed weak Sox2 expression in prosensory domain. When compared to E14.5 heterozygous controls, Sox2 expression was decreased by approximately 66% in *Six1enh21-Cre::Fgfr1^{lox/lox}* mutant cochlea, and by 49% in *Fgfr1^{ΔFrs/ΔFrs}*. Only a 12% decrease of Sox2 expression levels was observed in *Emx2-Cre::Fgfr1^{lox/lox}* mutants (Figure 10D). To exclude the possibility that reduced Sox2 expression was as a result of reduced cell numbers, Sox2-positive cells in the prosensory domain were counted (Figure 10E). No significant difference between controls (19.8 ± 1.5 ; $n = 5$) and both *Six1enh21-Cre::Fgfr1^{lox/lox}* (18 ± 1.0 ; $n = 4$) and *Fgfr1^{ΔFrs/ΔFrs}* (21.6 ± 1.5 ; $n = 4$) cochleae was detected. These results indicate that reduced expression of Sox2 is independent of cell number. In addition, reduced Sox2 expression was also detected in SCs of E18.5 *Fgfr1^{ΔFrs/ΔFrs}* cochlea (Figure 5G–I).

Sox2 expression in the sensory patch is induced by activation of the Notch receptor by its ligand *Jag1* [6,14]. Expression analysis of *Jag1* in *Six1enh21-Cre::Fgfr1^{lox/lox}* mutant revealed that its expression pattern is unchanged (Figure 11A and B), suggesting that FGFR1 signalling affects Sox2 expression independent of any affect on *Jag1* regulation. Taken together, we suggest that FGFR1-Frs2/3 signalling is required for Sox2 maintenance in sensory progenitors.

ERK phosphorylation is repressed in the inner ear of FGFR1 signalling mutants

Frs2/3-mediated FGFR1 signalling is transduced by a number of downstream pathways. We investigated which were activated during Sox2 maintenance in the sensory patch. The MAP kinase pathway is one of the key mediators of receptor tyrosine kinase signalling, and is activated through Frs2/3 recruitment to FGFR1 [25]. To determine if this pathway was activated in the inner ear, we used antibodies specific for the di-phosphorylated form of Erk1 and Erk2 (dpERK), an indicator of MAPK activity [33], to investigate the spatiotemporal activation of this pathway in the inner ear.

Our data thus far suggested that FGFR1 activity commencing prior to E12.5 and was necessary for Sox2 maintenance. In agreement with this timing, we detected ventral localization of dpErk in the otocyst of E10.5 *Fgfr1^{ΔFrs/+}* heterozygous embryos (Figure 12A). In contrast, otocyst expression could not be detected in homozygous *Fgfr1^{ΔFrs/ΔFrs}* embryos (Figure 12B). At E11.5, sections revealed ventromedial dpErk localization in the otocyst of *Six1enh21-Cre::Fgfr1^{lox/+}* heterozygous control (Figure 12C) but is down-regulated in both homozygous *Six1enh21-Cre::Fgfr1^{lox/lox}* otocyst as well as *Fgfr1^{ΔFrs/ΔFrs}* homozygote embryo (Figure 12D and E). Frs2/3-mediated FGFR1 signalling also activates PI3K, which results in the phosphorylation of Akt [26]. We thus asked if this pathway was also affected in FGFR1 signalling mutants. At

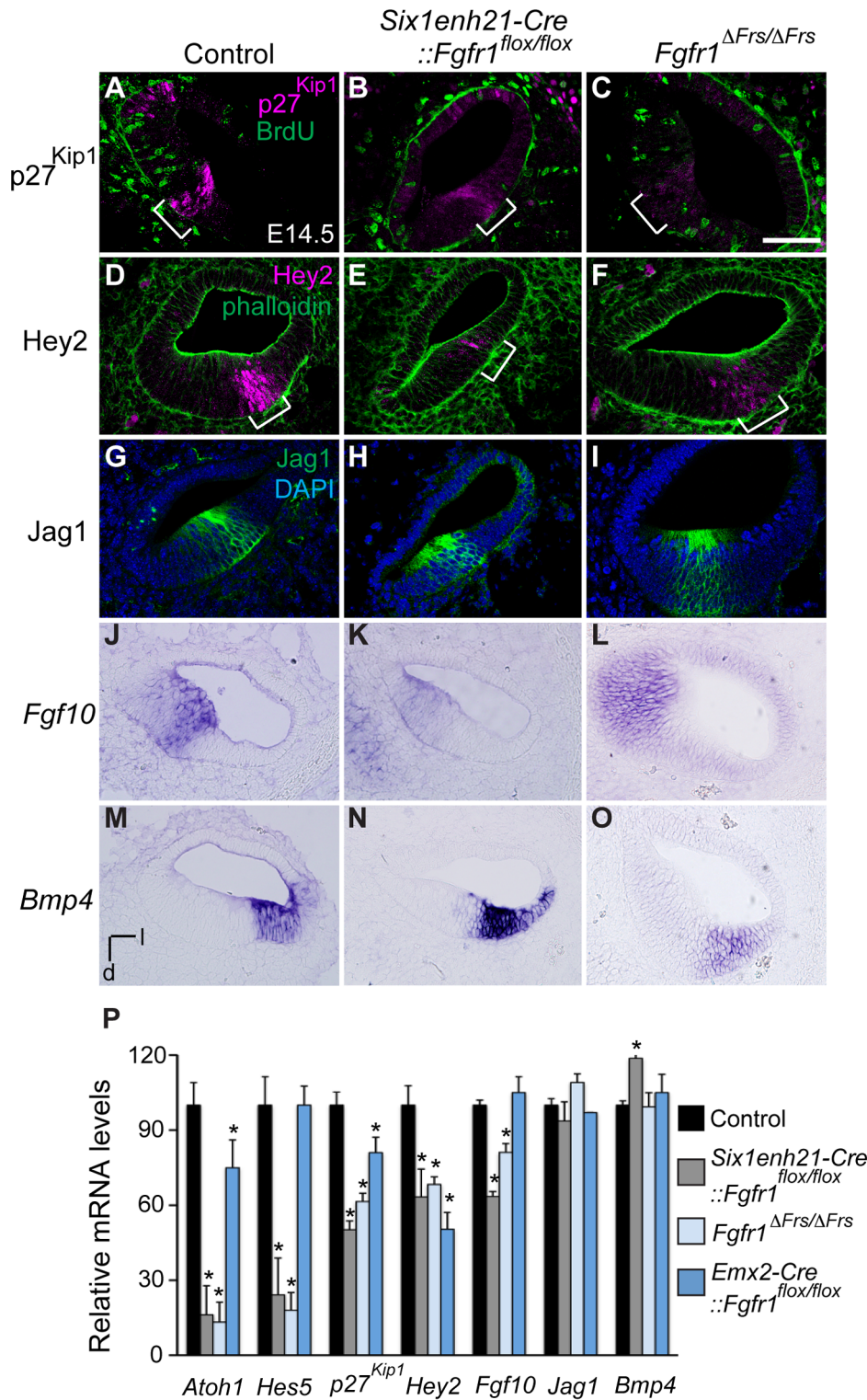


Figure 7. FGFR1-Frs2/3 pathway is required for the specification of prosensory domain. (A–C) p27^{Kip1} (magenta) is expressed in the post-mitotic, BrdU (green) negative, prosensory domain (bracket) in sections of E14.5 cochlea (A). Expression of p27^{Kip1} is decreased in *Six1enh21-Cre::Fgfr1^{flox/flox}* cochlea (B) and in *Fgfr1^{ΔFrs/ΔFrs}* cochlea (C). (D–F) Hey2 (magenta) is expressed in the prosensory domain (brackets) in sections of E14.5 cochlea (counter-stained with phalloidin: green) (D). Hey2 expression is down-regulated in both *Six1enh21-Cre::Fgfr1^{flox/flox}* mutant cochlea (E) and *Fgfr1^{ΔFrs/ΔFrs}* (F). (G–I) Section of control E14.5 cochlea shows Jag1 immuno-labelling in Kölliker’s organ. (G). Expression is unchanged in both *Six1enh21-Cre::Fgfr1^{flox/flox}* (H) and *Fgfr1^{ΔFrs/ΔFrs}* (I). (J–L) In situ hybridization of *Fgf10* on section of E14.5 cochlea shows expression in Kölliker’s organ (J). While the expression pattern is unchanged, *Fgf10* expression levels are lower in *Six1enh21-Cre::Fgfr1^{flox/flox}* cochlea (K). Expression in *Fgfr1^{ΔFrs/ΔFrs}* mutant cochlea is unchanged (L). (M–O) *Bmp4* expression in E14.5 control cochlea is restricted to the outer sulcus (M). The expression pattern is unchanged, however *Bmp4* expression levels are higher in *Six1enh21-Cre::Fgfr1^{flox/flox}* cochlea (N). Expression in *Fgfr1^{ΔFrs/ΔFrs}* mutant cochlea is unchanged (O). (P) Quantification of relative mRNA level of *Atoh1*, *Hes5*, p27^{Kip1}, *Hey2*, *Fgf10*, *Jag1* and *Bmp4* in E14.5 cochlear epithelial cells using quantitative PCR. Mean ± SD are shown. **p*<0.05. l, lateral; d, dorsal. Scale bar: A–O, 75 μm (in C). doi:10.1371/journal.pgen.1004118.g007

E12.5 we found no difference in the levels of phospho-Akt between *Six1enh21-Cre::Fgfr1^{lox/+}* heterozygous and *Six1enh21-Cre::Fgfr1^{lox/lox}* otocysts (Figure 12F).

At later stages of sensory cell development, FGF8 signalling mediated through FGFR3 is thought to play a role in the specification of pillar and Deiter's cells [34,35]. To verify the specificity of the FGFR1 signalling mutants, we asked if ERK phosphorylation was affected at these later stages. We found no obvious difference in dpErk localization to the cells of E14.5 *Six1enh21-Cre::Fgfr1^{lox/+}* heterozygous and *Six1enh21-Cre::Fgfr1^{lox/lox}* homozygous inner ears (Figure 12G and H), where nascent pillar cells IHCs are present. Thus, inhibition of signalling by FGFR1 specifically affects early ERK phosphorylation at E10.5 and E11.5, but does not affect later activation at E14.5 by other FGF receptors.

Discussion

Formation of cochlear HCs takes place progressively, with the potential of a group of Sox2-positive precursor cells, known as the sensory patch, becoming gradually restricted under the influence of a number of signalling molecules. Our observations suggest that FGFR1 signalling, acting through the adaptor Frs2/3, is responsible for sensory progenitor maintenance, partly through the maintenance of early Sox2 expression, and that in its absence, down-regulation of Sox2 results in a reduction in the number of HCs. However, despite the reduction of early Sox2 expression,

subsequent patterning of the sensory patch into the precursor domain of the sensory cells, the prosensory domain, is only partially affected. Surprisingly, even though prosensory domain markers such as p27^{Kip1} and Hey2 are dramatically down-regulated in both the conditional *Six1enh21-Cre::Fgfr1^{lox/lox}* and *Fgfr1^{ΔFrs/ΔFrs}* allele, a ZNPC is still established normally, and on schedule, showing the normal apical to basal progression. This also implies that the cell cycle inhibitor p27^{Kip1} is required redundantly for sensory progenitors to exit the cell cycle exit. In the mouse, the cell cycle inhibitor p19^{Ink4d} is also found in the sensory progenitors, and is known to act redundantly with p27^{Kip1} [36].

FGF signalling regulates Sox2 maintenance in the sensory patch

The regulation of Sox2 by FGF signaling has been characterized in a number of other systems, for example during foregut development [37], retinal pigmented epithelia [38], the lens placode [39] and in the differentiation of osteoblasts [40]. We show that in the cochlear precursor, FGF signalling maintains Sox2 expression.

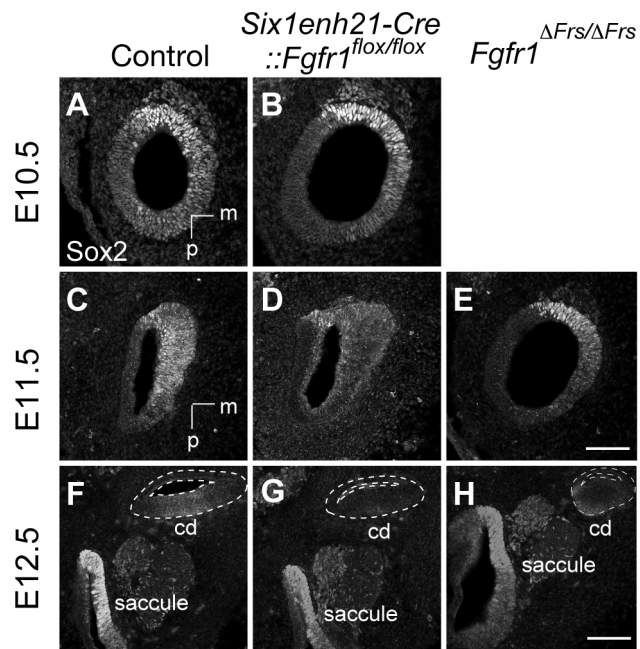


Figure 8. Sox2 is not maintained in FGFR1 signalling mutants. (A, B) Sox2 protein expression in sections of control E10.5 otocyst (A) is comparable to the expression observed in E10.5 *Six1enh21-Cre::Fgfr1^{lox/lox}* otocyst (B). (C–E) At E11.5, Sox2 expression is detected in the control otocysts (C), but is down-regulated in *Six1enh21-Cre::Fgfr1^{lox/lox}* otocyst sections (D). In *Fgfr1^{ΔFrs/ΔFrs}* otocyst, expression is slightly down-regulated, although the morphology of the otocyst is closer to E10.5 (E). (F–H) By E12.5, the cochlear duct expression of Sox2 is apparent in control inner ears (F), however Sox2 is down-regulated in *Six1enh21-Cre::Fgfr1^{lox/lox}* mutants (G) and *Fgfr1^{ΔFrs/ΔFrs}* inner ears (H) (within dotted lines). By contrast, Sox2 expression in saccular epithelium is unaffected in both mutants. m, medial; p, posterior; cd, cochlear duct. Scale bars: A–E; 75 μm (in E), F–H; 150 μm (in H). doi:10.1371/journal.pgen.1004118.g008

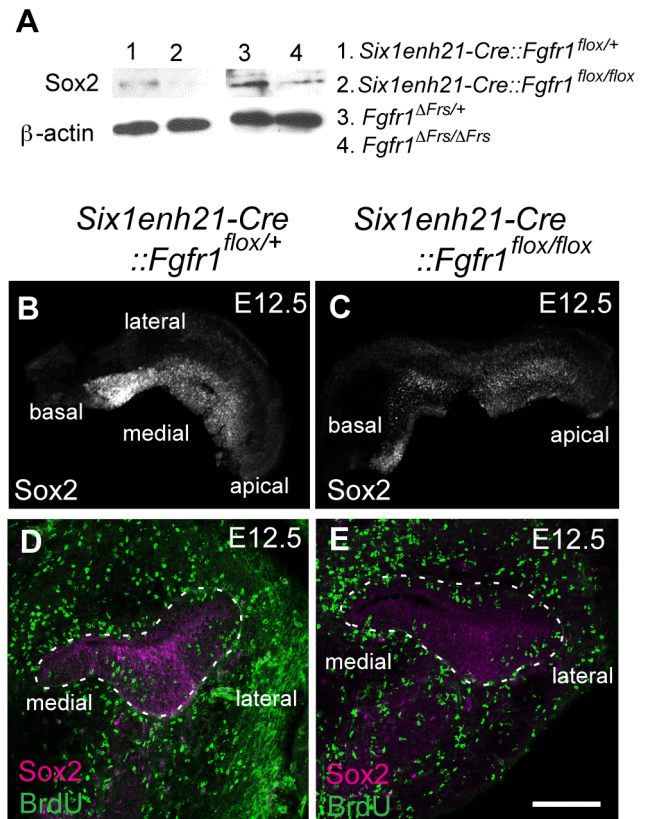


Figure 9. Sox2 is down-regulated prior to prosensory domain formation in FGFR1 signalling mutants. (A) Western blotting of cochlear lysates at E12.5 shows Sox2 protein in heterozygous *Six1enh21-Cre::Fgfr1^{lox/+}* (lane 1), mutant *Six1enh21-Cre::Fgfr1^{lox/lox}* (lane 2) or heterozygous *Fgfr1^{ΔFrs/+}* (lane 3), and mutant *Fgfr1^{ΔFrs/ΔFrs}* (lane 4). Sox2 is decreased in both FGFR1 signalling mutants compared to control. β-actin is used as a loading control. (B, C) Whole-mount cochlea at E12.5 show normal Sox2 expression in heterozygous controls (B), however Sox2 is down-regulated in *Six1enh21-Cre::Fgfr1^{lox/lox}* cochlea (C). (D, E) BrdU-positive cells are present along the width of cochlear duct of control (D) and *Six1enh21-Cre::Fgfr1^{lox/lox}* (E) (within dotted lines) although Sox2 immunoreactivity is decreased in the mutant cochlea. Scale bar: D, E, 75 μm (in E). doi:10.1371/journal.pgen.1004118.g009

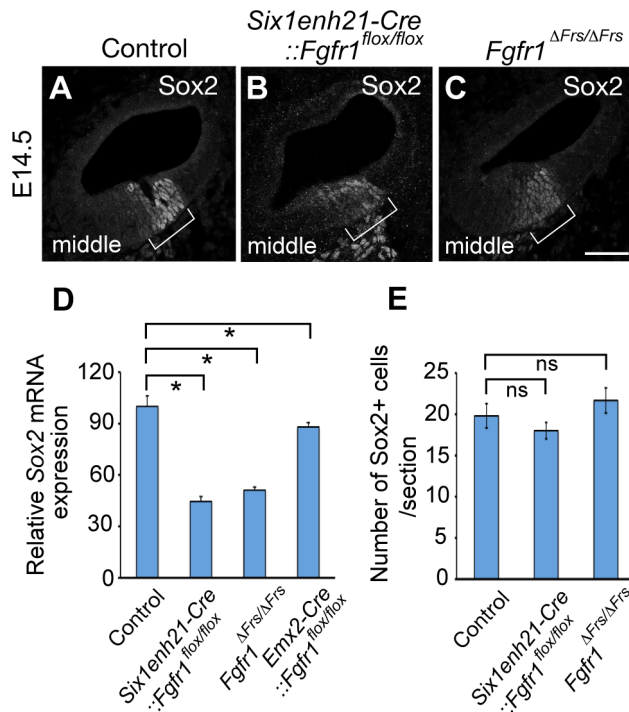


Figure 10. Sox2 is weakly expressed in FGFR1 signalling mutants at the onset of sensory cell differentiation. (A–C) At E14.5, Sox2 expression can be detected in the prosensory domain of control cochlear duct sections (A), but is down-regulated in *Six1enh21-Cre::Fgfr1^{flox/flox}* inner ear (B) and *Fgfr1^{ΔFrs/ΔFrs}* inner ears (C) (brackets). (D) Quantification of relative mRNA level of Sox2 in E14.5 cochlear epithelial cells using quantitative PCR. Mean \pm SD are shown. * $p < 0.05$. (E) The number of Sox2-positive cells from the middle turn of cochlear duct were counted. Mean \pm SD are shown. Scale bar: A–C; 75 μ m (in C). doi:10.1371/journal.pgen.1004118.g010

The reduction of Sox2 is not as a consequence of reduced proliferation (and hence reduced numbers) of Sox2-positive cells. While the number of proliferating cells in *Six1enh21-Cre::Fgfr1^{flox/flox}* cochlea is reduced, the numbers in the *Fgfr1^{ΔFrs/ΔFrs}* allele are not. Despite this difference, Sox2 levels are reduced in both mutants at E12.5 and E14.5, suggesting that during cochlear HC formation one role for FGFR1 signaling is in the maintenance of Sox2 expression. Further support for the regulation of Sox2 by FGFR1 signaling comes from the correspondence of HC loss seen in *Six1enh21-Cre::Fgfr1^{flox/flox}* and *Fgfr1^{ΔFrs/ΔFrs}* cochlea with other mutants. Sensory cell loss is more prominent apically in the cochlea, with the phenotype becoming milder basally. Such phenotypes are similar to knockouts or hypomorphic alleles of *Jag1* and *Sox2* [2,6], suggesting their involvement in a gene network with *Fgfr1*. Indeed further support for this molecular network comes from explant studies that show that exogenous application of FGF20 can overcome Notch-Jagged-mediated inhibition of Sox2 [22]. One caveat is that it is unclear whether the regulation of Sox2 maintenance by FGFR1 signalling is direct or indirect, through the upstream regulation of other factors important in Sox2 maintenance. It is clear that further studies are necessary to determine the exact mechanism by which FGFR1 signalling regulates Sox2.

At least two roles for Sox2 have been described during the formation of the cochlear sensory cells. The above-mentioned network, apparent from E10.5 to E12.5, maintains the competence of precursor cells to form sensory progenitors. This is

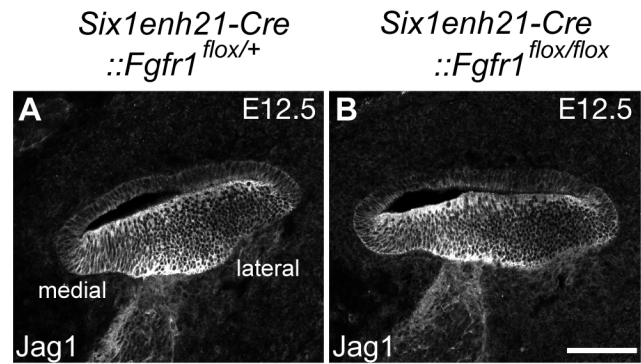


Figure 11. Sox2 down-regulation is independent of Jag1 action. (A, B) Expression of Jag1, the Notch ligand important for Sox2 expression, is unaffected in control (A) and *Six1enh21-Cre::Fgfr1^{flox/flox}* cochlea (B) at E12.5. Scale bar: A, B, 75 μ m in (B). doi:10.1371/journal.pgen.1004118.g011

supported by the analysis of the cochlear phenotype of mutant mice with little or no Sox2. These mutants show reduced, or absent HCs in the cochlea [2]. A later role for Sox2, from around E15, has been proposed. Here, Sox2 maintains SC fate, and preventing ectopic HC formation through the repression of *Atoh1* [4]. This is suggested by hypomorphic alleles where the reduction of Sox2 is not as severe. Here, HC number is increased [2,4]. Our results suggest that these two activities are separable, with FGFR1 signalling maintaining sensory commitment, partly through Sox2 regulation.

The question remains, how does decreased Sox2 as a result of reduced FGFR1 signalling translate into reduced sensory cells in the cochlea? Sox2 expression as well as other prosensory markers expressed in prosensory domain were down-regulated in both *Six1enh21-Cre::Fgfr1^{flox/flox}* and *Fgfr1^{ΔFrs/ΔFrs}* mutants, whereas only *Six1enh21-Cre::Fgfr1^{flox/flox}* mutants showed defect in cell proliferation. Moreover, both mutants showed similar effects on the formation of HCs. We thus conclude that early cell cycle exit provides, at most, a minor contribution to the disruption of prosensory formation, and hence cochlear HC development in FGFR1 signalling mutants. Instead, it is possible that the level or duration of Sox2 expression determines the commitment or competence to form HCs. A number of studies have described the quantitative requirement for Sox2 in other systems such as in the retinal progenitors [41], anterior foregut [37] and in taste buds [42]. Indeed, over-expression studies have suggested this is also the case in HC [4]. One possible mechanism, through which the duration of Sox2 expression in progenitors and precursors may be translated into effects on commitment and differentiation, is suggested from work on the effects of Sox2 binding to target gene enhancers in other systems [43,44]. Here silenced genes, important for cell type differentiation, are pre-bound with Sox2. Pre-binding is thought to be associated with the generation of local epigenetic changes [44] or is required for successive binding of co-operative factors [43], important in gene activation, priming the genes for activation. Consistent with this is data showing Sox2 binding sites in the *Atoh1*, a gene that is responsible for sensory cell differentiation in the inner ear [45]. Similarly, we suggest that one function of maintained early Sox2 expression, controlled by FGFR1 signalling, is to prime prosensory genes, such as *Atoh1*, for subsequent activation and thus control the differentiation of the sensory cells.

The disruption of the transition from Sox2-positive sensory progenitors to prosensory precursors also provides an explanation for the discontinuous “island” phenotype of HCs in the cochlea of FGFR1 signalling mutants. Convergent extension movements that

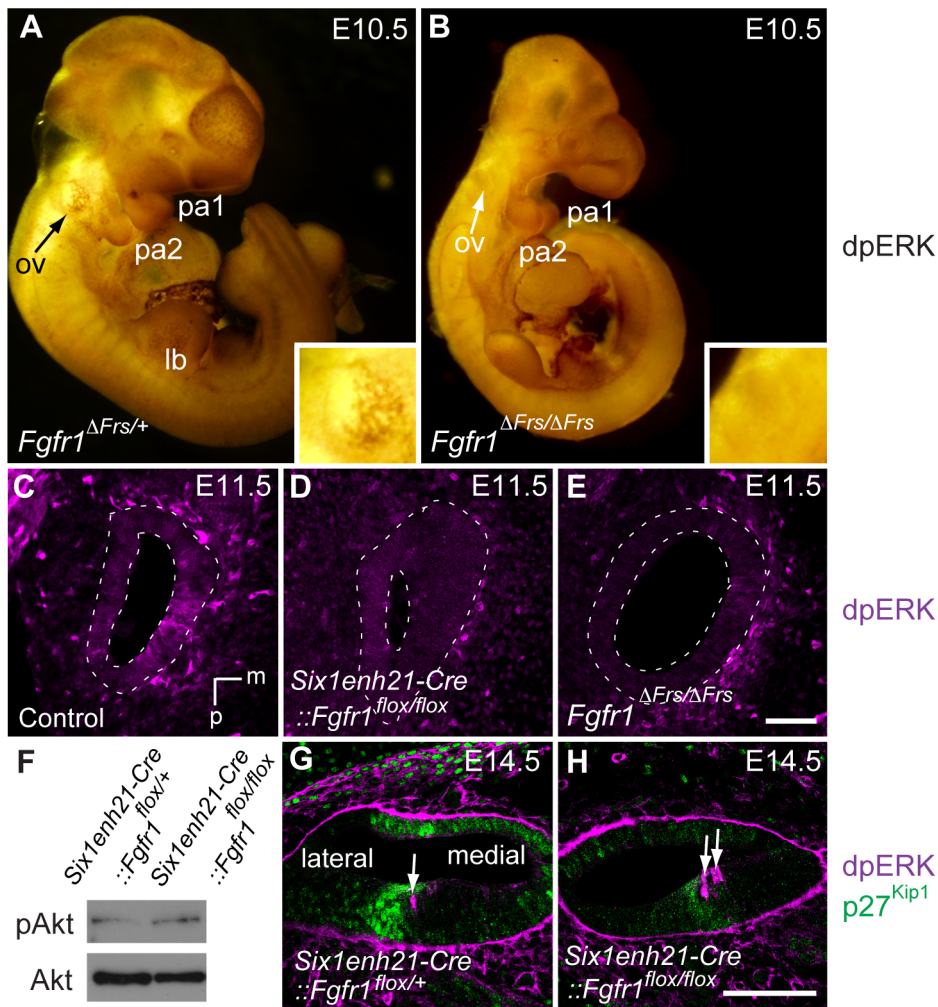


Figure 12. ERK phosphorylation is inhibited in the developing inner ear of FGFR1 signalling mutants. (A, B) Immunostaining for dpERK in E10.5 whole embryos, reveals ERK phosphorylation in the ventral half of the *Fgfr1*^{ΔFrs/+} otic vesicle (arrow, and inset for magnified image) (A). ERK phosphorylation is undetectable in mutant *Fgfr1*^{ΔFrs/ΔFrs} otocyst (arrow, and inset for magnified image) (B). For internal control, dpERK localization to rostral edge of PA1 and caudal edge of PA2 is detected in both heterozygotes and homozygotes. (C–E) dpERK immuno-labelling on coronal sections of E11.5 mouse heads. dpERK staining can be detected in the ventromedial wall of the control otocyst (C), but is undetectable in *Six1enh21-Cre::Fgfr1*^{fllox/fllox} (D) and *Fgfr1*^{ΔFrs/ΔFrs} otocysts (E) (dashed lines). (F) Western blotting was used to detect phosphorylated and unphosphorylated forms of Akt in protein extracted from E12.5 cochlear epithelia. The level of phosphorylated Akt was unchanged between *Six1enh21-Cre::Fgfr1*^{fllox/+} and *Six1enh21-Cre::Fgfr1*^{fllox/fllox} cochlea. (G, H) Immuno-labeling of cross sections of the cochlear duct of E14.5 mice with the dpERK and p27^{Kip1} antibodies. In both *Six1enh21-Cre::Fgfr1*^{fllox/+} (G) and *Six1enh21-Cre::Fgfr1*^{fllox/fllox} (H), the domain of dpERK (magenta) is localized to the medial border of prosensory domain marked by p27^{Kip1} (green) expression (arrows), where nascent IHC and inner pillar cells are present. m, medial; d, dorsal; ov, otic vesicle, pa, pharyngeal arch; lb, limb bud. Scale bars: C–E, 50 μm (in E); G, H, 75 μm (in H). doi:10.1371/journal.pgen.1004118.g012

partially drive cochlear extension normally distribute sensory precursors over the length of the organ of Corti [46,47]. However the fewer numbers of precursors in FGFR1 signalling mutants cannot be evenly dispersed. The apical to basal difference in the distribution of the sensory cells in these mutants may suggest directionality for these rearrangements.

FGFR1 signalling and inner ear hair cell development

Several studies have proposed FGF20 as the FGFR1 ligand during mouse cochlear development [21,48]. Indeed there is good correlation of the phenotype between *Fgf20*^{-/-} mutants and *Emx2-Cre::Fgfr1*^{fllox/fllox} described in this study; both have moderate reduction in the number of OHC, and IHC remains unaffected. In addition, their prosensory domain formation is largely unaffected. In contrast, there are important differences between *Fgf20* nulls

and both *Six1enh21-Cre::Fgfr1*^{fllox/fllox} and *Fgfr1*^{ΔFrs/ΔFrs} mutants. In these more severe *Fgfr1* mutants, HC number is more severely reduced and IHC are also affected. Analysis of *Fgf20* nulls revealed a function for Fgf20 in HC differentiation since undifferentiated Sox2-positive cells between sensory islands have been reported [21]. In *Fgfr1*^{ΔFrs/ΔFrs} mutant cochleae, however, there are no Sox2-positive cells detected in the lateral compartment among the HC islands. Furthermore, and in contrast to *Fgf20*^{-/-} mutant cochlea, Sox2 is down-regulated in both *Six1enh21-Cre::Fgfr1*^{fllox/fllox} and *Fgfr1*^{ΔFrs/ΔFrs} mutants from E12.5 to at least E14.5, and prosensory domain formation is disrupted. Our use of the two Cre drivers suggests a reason for this discrepancy. We propose that the FGFR1 has at least two distinct functions in auditory HC development. An early role, prior to E13.5, is in the maintenance of prosensory function, in part through the regulation of Sox2, and in the

development of IHC. A later role, in OHC development, is demonstrated by the use of *Emx2-Cre*, which only reaches the same level of driver activity as *Six1enh21-Cre* at E14.5. Here, Sox2 expression in prosensory domain is not severely affected despite significant reduction in OHC numbers. This suggests that a second Fgf ligand, operating either earlier or in combination with Fgf20, is required for the maintenance of Sox2. Although *Fgf20* is expressed in the sensory patches from E10.5 to E14.5 [21,22], it is likely that prosensory development, but not OHC development, could be compensated by the second ligand in *Fgf20*^{-/-} mutant cochlea. A number of Fgf ligands are expressed in the inner ear at these stages of development. *Fgf3*, -4, -5, -9, -10, -16, as well as *Fgf20* are all detected in the mammalian inner ear at early stages [21,48–54]. Receptor specificity can be used to narrow down the likely early ligand for FGFR1. It is known that mutation of the *Fgfr1-IIIb* isoform does not affect inner ear development, thus it is likely that the *Fgfr1-IIIc* isoform is operating in the sensory epithelium [20]. Of these 7 ligands, FGF4, -5, -9, -16, and FGF20 can bind and signal through FGFR1-IIIc [55,56], suggesting that one or more of these FGF molecules may act with FGF20 to maintain early *Sox2* expression.

FGF signalling triggers a downstream response, transducing external cues into an internal response. We find that in the absence of Fgfr1, or Frs2/3-mediated FGFR1 signalling, MAP kinase phosphorylation is attenuated, suggesting that this pathway is necessary for sensory progenitor maintenance. The similarity of the *Six1enh21-Cre::Fgfr1^{lox/lox}* phenotype with that of *Fgfr1^{ΔFrs/ΔFrs}* suggests that adaptor proteins Frs2/3 transduce the FGF signal during sensory progenitor maintenance. However there is an important difference between the two mutants. The defect in proliferation seen in *Six1enh21-Cre::Fgfr1^{lox/lox}* (and previously in *Foxg1-Cre::Fgfr1^{lox/lox}* [20]) is rescued in *Fgfr1^{ΔFrs/ΔFrs}*. This suggests the involvement of another downstream pathway in control proliferation in the cochlea. Indeed, the recovery of cell cycle impairment in *Fgfr1^{ΔFrs/ΔFrs}* is consistent with previous findings that cell lines obtained from *Fgfr1^{ΔFrs/ΔFrs}* are still capable of proliferating [28]. It is likely that other binding partners of FGFR1, such as Grb14, Crk, and Shc, which are known to regulate FGFR1-dependent cell proliferation may respond to mitogenic stimulation in the developing cochlea [57–59]. In contrast to the *Fgfr1^{ΔFrs/ΔFrs}*, which lacks the Frs2/3 interaction motif on FGFR1, mice carrying a point mutation in tyrosine at position 766, *Fgfr1^{Y766F/Y766F}* mice, showed no defect in inner ear development. Previous reports have suggested that Y766 phosphorylation may act to negatively regulate FGFR1 activity [30]. It is likely that FGFR1 activity is up-regulated in the inner ear of *Fgfr1^{Y766F/Y766F}* mutants. Given that previous studies have suggested that exogenous FGF ligands do not result in an obvious phenotype in the normal mouse cochlea [21], our observation of a normal cochlea in *Fgfr1^{Y766F/Y766F}* mice is not unreasonable.

Our analysis of a mutant of *Frs2* in which its subsequent binding to Shp2 is impaired (*Frs2α/2F*) revealed a very early defect in inner ear development, with the inner ear arrested at the otocyst stage (unpublished observations). This phenotype is more reminiscent of the *Fgfr2(IIIb)* mutant, which is thought to mediate signalling from Fgf3 and Fgf10 during inner ear induction [60]. This indicates that Frs2/3-mediated FGFR signalling, like FGF signalling itself, is iteratively employed during inner ear formation.

Materials and Methods

Ethics statement

Experiments were conducted and mice were housed, in accordance with local (RIKEN CDB) and national guidelines for animal experiments.

Generation of *Six1enh21-Cre* mice

Full details of the construction of *Six1enh21-Cre* mice will be presented elsewhere (S. S and K. K., in preparation). Briefly, a transgene was constructed in which the otic/epibranchial progenitor domain (OEPD) enhancer of the *Six1* homeobox gene (*Six1enh21*) [61] was placed upstream of Cre recombinase. Transgenic males were crossed with *Rosa26-flox-STOP-flox-eYFP* reporter females [62] and embryos were collected at stages E8.5 to E11.5. LacZ expression was found in the otic/epibranchial progenitor domain (OEPD) as early as E8.5. At subsequent stages (E9.5 to E11.5), LacZ expression was detected in the otic vesicle and epibranchial placodes/ganglia, scattered cells in the epibranchial ectoderm, the pharyngeal pouch endoderm as well as the olfactory placode/epithelium. The transgenic mouse line, m*Six1-21-NLSCre* (Acc. No. CDB0466T: <http://www.cdb.riken.jp/arg/TG%20mutant%20mice%20list.html>), and is available from the RIKEN BioResource Center (BRC).

Mice

Mice were housed in accordance with local and national guidelines for animal experiments. The *Fgfr1^{lox}* mutant mice have been described previously [20]. *Fgfr1^{Y766F}* mice were generated by crossing *Fgfr1^{n151F}* with the ubiquitously expressed Cre from *Ella-Cre* [30]. *Fgfr1^{ΔFrs}* mice have been previously described [28]. The *Rosa26-flox-STOP-flox-eYFP* was obtained from Jackson Laboratory (Bar Harbor, ME). The *Atoh1-GFP* line was provided by Dr. Jane Johnson [63]. *Emx2-Cre* mice were provided by Dr. Shinichi Aizawa [64]. *FoxG1-Cre* mice were provided by Jean Herbert, via Carina Hanashima [65]. *Frs2α^{2F/2F}* were as described previously [66].

Immunohistochemistry and histology

Staged mouse heads were fixed in 4% paraformaldehyde for 1–4.5 hours, depending on stage, and then prepared and mounted for cryo-sectioning. Immunofluorescence was performed as has previously been described [67]. The following antibodies were used: anti-p27^{Kip1} (#RB-006-P, Thermo Scientific, Fremont, CA), anti-Sox2 (#AB5603, Millipore, Temecula, CA), anti-pErk1/2 (#4370, Cell Signalling, Beverly, MA), anti-Hey2 (gifted by Neil Segil, House Ear Institute, Los Angeles, USA), anti-Prox1 (#AB5475, Millipore, Temecula, CA), anti-p75 (#AB1554, Millipore, Temecula, CA), anti-BrdU (#555627, BD Pharmingen, Franklin Lakes, NJ), anti-Jag1 (#sc-6011, Santa Cruz Biotechnology, Santa Cruz, CA), anti-GFP (#04406-26, Nacalai Tesque), anti-Caspase-3 (#G748A, Promega, Madison, WI), and anti-Myosin7a (#25-6790, Proteus, Ramona, CA). For BrdU staining, the specimens were pre-treated in 2N HCl for 20 min at 37°C, and neutralized with 0.01M PBS (pH 8.5) for 10 min at room temperature. For whole-embryo dpERK staining, fixed embryos were dehydrated in a graded methanol series and then treated with 5% H₂O₂ for 1 hr. Rehydrated embryos were processed as previously described [68]. Signal was detected using DAB substrate kit for peroxidase (Vector). Alexa-488, Alexa-594, or anti-rabbit-HRP (Dako) conjugated secondary antibodies were used to detect primary antibodies. F-actin was detected using phalloidin conjugated to Alexa-488 (Molecular Probes).

Cell counting and measurement of cochlear length

For cochlear and vestibular HC counting, E16.5–E18.5 samples stained with Myo7a or expressing *Atoh1-GFP* were used since most *Fgfr1* mutants die before birth. Inner and outer HC were distinguished by location and morphology as described previously [21]. Group of single row of HCs was regarded as IHCs since they

were located medial side of p75-expressing pillar cells. Relative cochlear length was measured using ImageJ software. For evaluation of HC number per length, we counted more than 300 μm regions of the base, middle, and apex of the cochlea and normalized counts to 100 μm (more than $n = 4$ in each HC type) as described [21]. For Sox2-positive cell counting, cross sections from E14.5 samples were made and middle turn of cochlear duct stained with anti-Sox2 antibody was chosen.

RNA *in situ* hybridization

RNA *in situ* hybridization on cryo-sections was performed as previously described [69].

Paint-filling

The gross anatomy of bony labyrinths at E14.5 was visualized by paint-filling as previously described [29]. Briefly, decapitated heads were fixed in Bodian's fixative over night. Specimens were subsequently immersed in a graded ethanol series to dehydrate, and cleared in a 2:1 mixture of benzyl benzoate and benzoic acid (BABB). The inner ears were visualized by injection of 1% white paint in BABB into the common crus.

Bromo-deoxyuridine incorporation assay

BrdU (100 mg/g body weight) was injected into pregnant mice intra-peritoneally at E10.5–E14.5. BrdU injected mice were sacrificed 2 hours after injection, and then fixed in 4% PFA. BrdU-positive cells were counted in at least four cross sections of the cochlear apical (at E12.5) or middle (at E14.5) turn. For E14.5 samples, only BrdU-labelled cells in Kölliker's organ were counted. Data shown are mean \pm SD. P-values were calculated using unpaired t-test, to determine the significance of the difference between experimental and control samples.

Quantitative reverse transcription PCR

Whole otocyst or cochlear epithelial cells were dissected from embryos at E10.5–E14.5 (at least $n = 2$ in each sample). Enzymatic treatment was conducted to remove mesenchyme [70]. Total RNA from pure otic epithelial cells was extracted using the RNAqueous-Micro kit (#AM1931, Ambion, Austin, TX) and then reverse-transcribed using First Strand cDNA Synthesis Kit for RT-PCR (#11483188001, Roche, Indianapolis, IN). Synthesized cDNA and primer sets were mixed with Power SYBR Green

PCR Master Mix (#4367669, Applied Biosystems, Warrington, UK), and real-time quantitative PCR was performed using an ABI Prism 7900 Sequence Detection System (Applied Biosystems). All reactions were carried out in duplicate. The relative amount of mRNA was calculated by standard curve method, and normalized to that of 36B4 mRNA [71]. P-values were calculated using unpaired t-test, to determine the significance of the difference between experimental and control samples.

Immunoblotting

E12.5 or E14.5 cochlear epithelial cells, purified from underlying mesenchymal cells were lysed in a buffered solution, consisting of SDS, salt, phosphatase inhibitor, and proteinase inhibitor. A mixture of lysate, sample buffer, and 2-mercaptoethanol, were boiled at 98°C for 2 min and separated on a SuperSep Ace gel (Wako), and subsequently transferred into PVDF membrane (GE Healthcare). The following antibodies were used: rabbit anti-Akt antibody (1: 1000) (#9272, Cell Signalling Technology), anti-Sox2 (1: 1000) (#AB5603, Millipore, Temecula, CA), rabbit anti-Phospho Akt antibody (1: 1000) (#9271, Cell Signalling Technology), and anti-Actin antibody (1: 10000) (MBL). Horseradish peroxidase-linked anti-rabbit IgGs were used as secondary antibodies (1:10,000) (GE Healthcare) and revealed using Amersham ECL Prime Western Blotting Detection Reagent (GE Healthcare) according to the manufacturer's instruction. ImageJ software was used to compare the relative Sox2 protein amount between control and *Fgfr1* mutants.

Acknowledgments

We thank members of the Lab for Sensory Development for comments throughout this study. We are grateful to Phillippe Soriano for the *Fgfr1* ^{Δ Fr5} ES cells, Shinichi Aizawa for the *Emx2-Cre* mice, Juha Partanen for the *Fgfr1*^{flac} and *Fgfr1*^{fl51F} mice, Jane Johnson for *Atoh1-GFP* mice, and the CDB's Animal Facility for their excellent maintenance of these mice. This paper is dedicated to the memory of Kanako Ota.

Author Contributions

Conceived and designed the experiments: KO TK RKL. Performed the experiments: KO TK PO SSM MP. Analyzed the data: KO TK YS RKL. Contributed reagents/materials/analysis tools: SS MI NG KK. Wrote the paper: KO RKL.

References

- Groves AK, Fekete DM (2012) Shaping sound in space: the regulation of inner ear patterning. *Development* 139: 245–257.
- Kiernan AE, Pelling AL, Leung KK, Tang AS, Bell DM, et al. (2005) Sox2 is required for sensory organ development in the mammalian inner ear. *Nature* 434: 1031–1035.
- Neves J, Kamaid A, Alsina B, Giraldez F (2007) Differential expression of Sox2 and Sox3 in neuronal and sensory progenitors of the developing inner ear of the chick. *J Comp Neurol* 503: 487–500.
- Dabdoub A, Puligilla C, Jones JM, Fritsch B, Cheah KS, et al. (2008) Sox2 signaling in prosensory domain specification and subsequent hair cell differentiation in the developing cochlea. *Proc Natl Acad Sci U S A* 105: 18396–18401.
- Daudet N, Lewis J (2005) Two contrasting roles for Notch activity in chick inner ear development: specification of prosensory patches and lateral inhibition of hair-cell differentiation. *Development* 132: 541–551.
- Kiernan AE, Xu J, Gridley T (2006) The Notch Ligand JAG1 Is Required for Sensory Progenitor Development in the Mammalian Inner Ear. *PLoS Genet* 2: e4.
- Daudet N, Ariza-McNaughton L, Lewis J (2007) Notch signalling is needed to maintain, but not to initiate, the formation of prosensory patches in the chick inner ear. *Development* 134: 2369–2378.
- Hartman BH, Reh TA, Bermingham-McDonogh O (2010) Notch signaling specifies prosensory domains via lateral induction in the developing mammalian inner ear. *Proc Natl Acad Sci U S A* 107: 15792–15797.
- Neves J, Parada C, Chamizo M, Giraldez F (2011) Jagged 1 regulates the restriction of Sox2 expression in the developing chicken inner ear: a mechanism for sensory organ specification. *Development* 138: 735–744.
- Ohyama T, Basch ML, Mishina Y, Lyons KM, Segil N, et al. (2010) BMP signaling is necessary for patterning the sensory and nonsensory regions of the developing mammalian cochlea. *J Neurosci* 30: 15044–15051.
- Chen P, Segil N (1999) p27(Kip1) links cell proliferation to morphogenesis in the developing organ of Corti. *Development* 126: 1581–1590.
- Lee YS, Liu F, Segil N (2006) A morphogenetic wave of p27Kip1 transcription directs cell cycle exit during organ of Corti development. *Development* 133: 2817–2826.
- Lanford PJ, Lan Y, Jiang R, Lindsell C, Weinmaster G, et al. (1998) Cell fate choices and the expression of Notch, Delta and Serrate homologues in the chick inner ear: parallels with *Drosophila* sense-organ development. *Development* 125: 4645–4654.
- Brooker R, Hozumi K, Lewis J (2006) Notch ligands with contrasting functions: Jagged1 and Delta1 in the mouse inner ear. *Development* 133: 1277–1286.
- Adam J, Myat A, Le Roux I, Eddison M, Henrique D, et al. (1998) Notch signalling pathway mediates hair cell development in mammalian cochlea. *Nat Genet* 21: 289–292.
- Woods C, Montcouquiol M, Kelley MW (2004) Math1 regulates development of the sensory epithelium in the mammalian cochlea. *Nat Neurosci* 7: 1310–1318.
- Driver EC, Sillers L, Coate TM, Rose MF, Kelley MW (2013) The *Atoh1*-lineage gives rise to hair cells and supporting cells within the mammalian cochlea. *Dev Biol* 376: 86–98.

18. Bermingham NA, Hassan BA, Price SD, Vollrath MA, Ben-Arie N, et al. (1999) Math1: an essential gene for the generation of inner ear hair cells. *Science* 284: 1837–1841.
19. Chen P, Johnson JE, Zoghbi HY, Segal N (2002) The role of Math1 in inner ear development: Uncoupling the establishment of the sensory primordium from hair cell fate determination. *Development* 129: 2495–2505.
20. Pirvola U, Ylikoski J, Trokovic R, Hebert JM, McConnell SK, et al. (2002) FGFR1 is required for the development of the auditory sensory epithelium. *Neuron* 35: 671–680.
21. Huh SH, Jones J, Warchol ME, Ornitz DM (2011) Differentiation of the lateral compartment of the cochlea requires a temporally restricted FGF20 signal. *PLoS Biol* 10: e1001231.
22. Munnamalai V, Hayashi T, Bermingham-McDonogh O (2012) Notch prosensory effects in the Mammalian cochlea are partially mediated by Fgf20. *J Neurosci* 32: 12876–12884.
23. Turner N, Grose R (2010) Fibroblast growth factor signalling: from development to cancer. *Nat Rev Cancer* 10: 116–129.
24. Mohammadi M, Dionne CA, Li W, Li N, Spivak T, et al. (1992) Point mutation in FGF receptor eliminates phosphatidylinositol hydrolysis without affecting mitogenesis. *Nature* 358: 681–684.
25. Kouhara H, Hadari YR, Spivak-Kroizman T, Schilling J, Bar-Sagi D, et al. (1997) A lipid-anchored Grb2-binding protein that links FGF-receptor activation to the Ras/MAPK signaling pathway. *Cell* 89: 693–702.
26. Ong SH, Hadari YR, Gotoh N, Guy GR, Schlessinger J, et al. (2001) Stimulation of phosphatidylinositol 3-kinase by fibroblast growth factor receptors is mediated by coordinated recruitment of multiple docking proteins. *Proc Natl Acad Sci U S A* 98: 6074–6079.
27. Gotoh N (2008) Regulation of growth factor signaling by FRS2 family docking/scaffold adaptor proteins. *Cancer Sci* 99: 1319–1325.
28. Hoch RV, Soriano P (2006) Context-specific requirements for Fgfr1 signaling through Frs2 and Frs3 during mouse development. *Development* 133: 663–673.
29. Morsli H, Choo D, Ryan A, Johnson R, Wu DK (1998) Development of the mouse inner ear and origin of its sensory organs. *J Neurosci* 18: 3327–3335.
30. Partanen J, Schwartz L, Rossant J (1998) Opposite phenotypes of hypomorphic and Y766 phosphorylation site mutations reveal a function for Fgfr1 in anteroposterior patterning of mouse embryos. *Genes Dev* 12: 2332–2344.
31. Bermingham-McDonogh O, Oesterle EC, Stone JS, Hume CR, Huynh HM, et al. (2006) Expression of Prox1 during mouse cochlear development. *J Comp Neurol* 496: 172–186.
32. Ahmed M, Wong EY, Sun J, Xu J, Wang F, et al. (2012) Eya1-Six1 interaction is sufficient to induce hair cell fate in the cochlea by activating Atoh1 expression in cooperation with Sox2. *Dev Cell* 22: 377–390.
33. Yung Y, Dolginov Y, Yao Z, Rubinfeld H, Michael D, et al. (1997) Detection of ERK activation by a novel monoclonal antibody. *FEBS Lett* 408: 292–296.
34. Jacques BE, Montcouquiol ME, Layman EM, Lewandoski M, Kelley MW (2007) Fgf8 induces pillar cell fate and regulates cellular patterning in the mammalian cochlea. *Development* 134: 3021–3029.
35. Hayashi T, Cunningham D, Bermingham-McDonogh O (2007) Loss of Fgfr3 leads to excess hair cell development in the mouse organ of Corti. *Dev Dyn* 236: 525–533.
36. Chen P, Zindy F, Abdala C, Liu F, Li X, et al. (2003) Progressive hearing loss in mice lacking the cyclin-dependent kinase inhibitor Ink4d. *Nat Cell Biol* 5: 422–426.
37. Que J, Okubo T, Goldenring JR, Nam KT, Kurotani R, et al. (2007) Multiple dose-dependent roles for Sox2 in the patterning and differentiation of anterior foregut endoderm. *Development* 134: 2521–2531.
38. Ishii Y, Weinberg K, Oda-Ishii I, Coughlin L, Mikawa T (2009) Morphogenesis and cytodifferentiation of the avian retinal pigmented epithelium require downregulation of Group B1 Sox genes. *Development* 136: 2579–2589.
39. Takemoto T, Uchikawa M, Kamachi Y, Kondoh H (2006) Convergence of Wnt and FGF signals in the genesis of posterior neural plate through activation of the Sox2 enhancer N-1. *Development* 133: 297–306.
40. Mansukhani A, Ambrosetti D, Holmes G, Cornivelli L, Basilico C (2005) Sox2 induction by FGF and FGFR2 activating mutations inhibits Wnt signaling and osteoblast differentiation. *J Cell Biol* 168: 1065–1076.
41. Taranova OV, Magness ST, Fagan BM, Wu Y, Surzenko N, et al. (2006) SOX2 is a dose-dependent regulator of retinal neural progenitor competence. *Genes Dev* 20: 1187–1202.
42. Okubo T, Pevny LH, Hogan BL (2006) Sox2 is required for development of taste bud sensory cells. *Genes Dev* 20: 2654–2659.
43. Bergsland M, Ramskold D, Zaouter C, Klum S, Sandberg R, et al. (2011) Sequentially acting Sox transcription factors in neural lineage development. *Genes Dev* 25: 2453–2464.
44. Liber D, Domaschek R, Holmqvist PH, Mazzarella L, Georgiou A, et al. (2010) Epigenetic priming of a pre-B cell-specific enhancer through binding of Sox2 and Foxd3 at the ESC stage. *Cell Stem Cell* 7: 114–126.
45. Neves J, Uchikawa M, Bigas A, Giraldez F (2012) The prosensory function of Sox2 in the chicken inner ear relies on the direct regulation of Atoh1. *PLoS One* 7: e30871.
46. Jones C, Chen P (2007) Planar cell polarity signaling in vertebrates. *Bioessays* 29: 120–132.
47. Yamamoto N, Okano T, Ma X, Adelstein RS, Kelley MW (2009) Myosin II regulates extension, growth and patterning in the mammalian cochlear duct. *Development* 136: 1977–1986.
48. Hayashi T, Ray CA, Bermingham-McDonogh O (2008) Fgf20 is required for sensory epithelial specification in the developing cochlea. *J Neurosci* 28: 5991–5999.
49. Kawakami T, Kawcak T, Li YJ, Zhang W, Hu Y, et al. (2002) Mouse dispatched mutants fail to distribute hedgehog proteins and are defective in hedgehog signaling. *Development* 129: 5753–5765.
50. Pirvola U, Zhang X, Mantela J, Ornitz DM, Ylikoski J (2004) Fgf9 signaling regulates inner ear morphogenesis through epithelial-mesenchymal interactions. *Dev Biol* 273: 350–360.
51. Wright TJ, Hatch EP, Karabaghi H, Karabaghi P, Schoenwolf GC, et al. (2003) Expression of mouse fibroblast growth factor and fibroblast growth factor receptor genes during early inner ear development. *Dev Dyn* 228: 267–272.
52. Wright TJ, Mansour SL (2003) Fgf3 and Fgf10 are required for mouse otic placode induction. *Development* 130: 3379–3390.
53. Hatch EP, Noyes CA, Wang X, Wright TJ, Mansour SL (2007) Fgf3 is required for dorsal patterning and morphogenesis of the inner ear epithelium. *Development* 134: 3615–3625.
54. Kumar M, Chapman SC (2012) Cloning and expression analysis of Fgf5, 6 and 7 during early chick development. *Gene Expr Patterns* 12: 245–253.
55. Ornitz DM, Xu J, Colvin JS, McEwen DG, MacArthur CA, et al. (1996) Receptor specificity of the fibroblast growth factor family. *J Biol Chem* 271: 15292–15297.
56. Zhang X, Ibrahim OA, Olsen SK, Umemori H, Mohammadi M, et al. (2006) Receptor specificity of the fibroblast growth factor family. The complete mammalian FGF family. *J Biol Chem* 281: 15694–15700.
57. Reilly JF, Mickey G, Maher PA (2000) Association of fibroblast growth factor receptor 1 with the adaptor protein Grb14. Characterization of a new receptor binding partner. *J Biol Chem* 275: 7771–7778.
58. Dunican DJ, Williams EJ, Howell FV, Doherty P (2001) Selective inhibition of fibroblast growth factor (FGF)-stimulated mitogenesis by a FGF receptor-1-derived phosphopeptide. *Cell Growth Differ* 12: 255–264.
59. Larsson H, Klint P, Landgren E, Claesson-Welsh L (1999) Fibroblast growth factor receptor-1-mediated endothelial cell proliferation is dependent on the Src homology (SH) 2/SH3 domain-containing adaptor protein Crk. *J Biol Chem* 274: 25726–25734.
60. Pirvola U, Spencer-Dene B, Xing-Qun L, Kettunen P, Thesleff I, et al. (2000) FGF/FGFR-2(IIIb) signaling is essential for inner ear morphogenesis. *J Neurosci* 20: 6125–6134.
61. Sato S, Ikeda K, Shioi G, Nakao K, Yajima H, et al. (2012) Regulation of Six1 expression by evolutionarily conserved enhancers in tetrapods. *Dev Biol* 368: 95–108.
62. Soriano P (1999) Generalized lacZ expression with the ROSA26 Cre reporter strain. *Nat Genet* 21: 70–71.
63. Lumpkin EA, Collisson T, Parab P, Omer-Abdalla A, Haerberle H, et al. (2003) Math1-driven GFP expression in the developing nervous system of transgenic mice. *Gene Expr Patterns* 3: 389–395.
64. Kimura J, Suda Y, Kurokawa D, Hossain ZM, Nakamura M, et al. (2005) Emx2 and Pax6 function in cooperation with Otx2 and Otx1 to develop caudal forebrain primordium that includes future archipallium. *J Neurosci* 25: 5097–5108.
65. Hebert JM, McConnell SK (2000) Targeting of cre to the Foxg1 (BF-1) locus mediates loxP recombination in the telencephalon and other developing head structures. *Dev Biol* 222: 296–306.
66. Yamamoto S, Yoshino I, Shimazaki T, Murohashi M, Hevner RF, et al. (2005) Essential role of Shp2-binding sites on FRS2alpha for corticogenesis and for FGF2-dependent proliferation of neural progenitor cells. *Proc Natl Acad Sci U S A* 102: 15983–15988.
67. Teraoka ME, Paschaki M, Muta Y, Ladher RK (2009) Rostral paraxial mesoderm regulates refinement of the eye field through the bone morphogenetic protein (BMP) pathway. *Dev Biol* 330: 389–398.
68. Lunn JS, Fishwick KJ, Halley PA, Storey KG (2007) A spatial and temporal map of FGF/Erk1/2 activity and response repertoires in the early chick embryo. *Dev Biol* 302: 536–552.
69. O'Neill P, Mak SS, Fritsch B, Ladher RK, Baker CV (2012) The amniote paratympanic organ develops from a previously undiscovered sensory placode. *Nat Commun* 3: 1041.
70. Sakamoto T, Ito J, Ladher RK (2007) Hair cell differentiation becomes tissue specific by E9.5 in mouse inner ear. *Neuroreport* 18: 841–844.
71. Yamamoto N, Chang W, Kelley MW (2011) Rbpj regulates development of prosensory cells in the mammalian inner ear. *Dev Biol* 353: 367–379.